ESTER SYNTHESIS THROUGH COBALT-CATALYZED DEHYDROGENATIVE COUPLING OF PRIMARY ALCOHOLS

By

Oluwadamilola Oyewole

A Thesis Submitted in Partial Fulfillment of the Requirements for the Degree

of Master of Science in Chemistry

Middle Tennessee State University

November 2024

Thesis Committee:

Dr. Keying Ding, Chair

Dr. Jing Kong

Dr. Chengshan Wang

Dedicated to the memory of Mrs. Gloria Adeyemi, my beloved big mommy, and Opeyemi Oladele, my dear friend. Rest in Peace. Your memory lives on.

ABSTRACT

The search for sustainable alternatives to precious metal catalysts has become increasingly vital in modern chemistry. A groundbreaking solution emerges through the application of first-row transition metals combined with pincer ligands, offering both economic and environmental advantages. Our research introduces ^{iPr}PPPBF, a novel phosphine-based ligand incorporating a benzofuran scaffold, which was synthesized under carefully controlled conditions. Through meticulous crystallization procedures, we obtained pure ligand samples that were subsequently complexed with cobalt. Advanced X-ray crystallography revealed the detailed molecular structures of these metal complexes. The cobalt variant demonstrated remarkable catalytic efficiency in transforming benzyl alcohol into its corresponding benzoate ester through dehydrogenative coupling. This achievement marks a significant advancement in developing sustainable catalytic systems, suggesting broader applications in alcohol functionalization reactions. Our findings contribute to the growing field of earth-abundant metal catalysis, offering more sustainable alternatives to traditional precious metal systems throughout modern industrial chemistry processes and future green synthesis methodologies.

TABLE OF CONTENTS

LIST OF FIGURES

LIST OF SCHEMES

LIST OF TABLES

CHAPTER 1
INTRODUCTION

1.1 Ester Production

Chemists extensively study esters and use them as intermediates and products in many branches of the chemical industry.[1,2] Combining and altering them allows chemists to create many materials with characteristics. For example, polyester is a polymer based on ester monomers used to produce textiles, polymers, and resins. They play a vital role as precursors for constructing more complex substances, including agrochemicals, drugs, and materials with desirable physical and chemical properties.

Esters are significant to the fragrance business because of their characteristic and frequently pleasant smells. Many natural esters are present as components of the fragrance of fruits and flowers, for example, ethyl salicylate in wintergreen and butyl butyrate in pineapples. To create beautiful and exciting smells or replace them in their formation process, perfumers skillfully combine several esters. Because these molecules can be synthesized, perfumes can be produced consistently without depending on natural sources, which can be limited and affected by environmental variables.

Esters are also widely used in the flavor industry to develop and improve food flavors. Certain esters make up most of many fruit flavors.[1,2] For instance, isoamyl acetate gives banana flavor, while ethyl acetate imparts flavors to fruits and wine. It is still important to note that the food

industry uses many esters' high volatility and low toxicity to create lasting, safe flavoring compounds that can be applied to any product, from beverages and baked goods to candies and processed foods.

Esters have many application areas in many industries. Many drugs in the pharmaceutical sector contain ester functional groups, which may affect the drug products' pharmacokinetics, stability, and bioavailability. An ester of salicylic acid is aspirin. Esters are also utilized to synthesize biodiesel, a renewable diesel fuel made from fatty acid esters extracted from vegetable or animal fats rather than petroleum.

Cosmetic products are also produced using esters, which are significant industry products. Some skin care emollients and moisturizers are esters, which are preferred because of their skin-smoothing property, but they are non-greasy. The esters synthesized are used to prepare many cosmetic products appropriate for various skin types.

Esters, due to their non-polar nature, are used in industrial processing as solvents, plasticizers, and lubrication. They are widely used in manufacturing processes within most electronics and automobile industries. For instance, ester-based solvents are used because they are non-toxic, and biodegradable compared to certain petroleum-based solvents.

Another significant aspect of ester production is in material science's research and development area. Esters are a perfect example of how a regular organic group can significantly affect different industries and people's lives. Every waking moment, from the clothes we wear and

the colognes or perfumes we put on to the food we consume, including the medicines we take, esters go unnoticed, but they are indispensable in our day-to-day lives. More exciting results are expected in chemistry and related fields by their continued study and application.

1.1.1 Conventional Ester Production Methods

In the past, esters have been produced in several ways like esterification of carboxylic acids with alcohol, alcoholysis of acyl chloride and acid anhydride, carbonylation of alkenes by alcohol, transesterification, along with others.[1,2] They are effective methods but suffer from certain drawbacks from the environmental angle of view. These can involve severe reaction conditions, yield large volumes of by-products, or utilize toxic reactants or a catalyst.

For example, the Fischer esterification reaction between a carboxylic acid and alcohol generally uses strong acid catalysts. Usually, it has to be forced to yield an excellent product by removing water, a co-product of a reaction. This process can be energy-consuming and may lead to acidic wastewater forming, which needs to be treated before discharge /disposal. Likewise, acyl chlorides are highly reactive species for forming esters but generate hydrochloric acid, a corrosive and ecologically sensitive chemical substance.

Also, the overall response of dimethyl carbonate (DMC) as a methylating agent is depicted in Scheme 1.1. It shows how several chemicals (ROH, RNH_2, RCOOH, RCH_2CN) can be methylated with DMC for the esterification of carboxylic acids, yielding CO_2 and methanol as byproducts.

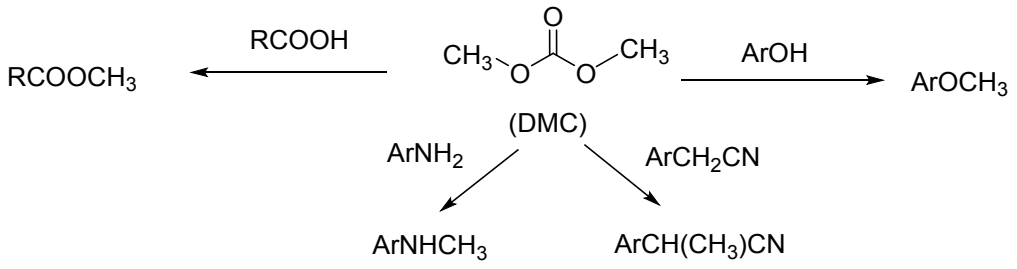

Scheme 1.1 Methylation of phenols, anilines, and activated methylenes[3]

In modern chemistry, the effects of CO_2 and methanol on the environment are significant problems. One major greenhouse gas that significantly contributes to climate change and global warming is CO_2.[4] Marine habitats are at risk due to ocean acidification brought on by its rising atmospheric concentration.[5] Methanol is hazardous to terrestrial and aquatic habitats, even though it is less persistent than CO_2. When discharged into the atmosphere, its toxicity can cause harm to a variety of creatures and play a role in creating ground-level ozone.[6] These environmental factors highlight how crucial it is to create green chemistry techniques that reduce the creation and discharge of these pollutants.

1.1.2 The Green Chemistry Paradigm

The idea of green chemistry, which started in the early 1990s, has provided a turning point for chemical synthesis and process development. These principles stress banning waste, maximizing atomic efficiency, using energy-efficient processes, and using greener solvents and reagents. These principles have been applied in ester production to change the research towards environmentally friendly methods.

1.1.2.1 Dehydrogenative Coupling Reactions

Of these, the acceptorless oxidant-free dehydrogenative coupling of alcohols emerges as a highly effective strategy. This method represents a significant step forward in green chemistry for several reasons:

- **Atom Economy:** It is a very ‘atom-economical’ reaction. This efficiency reduces wastage right from the molecular level of an economy.
- **Byproduct:** The only unwanted product formed in this reaction is hydrogen gas, which is, in any case, a safe gas. Hydrogen is widely used in industrial applications to convert different substances and is gradually considered a type of renewable energy source.
- **Oxidant-Free:** This approach is oxidant-free in contrast to most conventional oxidation reactions, which employ equimolar amounts of often toxic or corrosive oxidant reagents. This removal of oxidizing agents also has a dramatic effect in reducing the environmental burden of the process.
- **Starting Materials:** The method operates with alcohols as primary reagents, which, as a rule, are easier to obtain, biorenewable feedstock and less toxic than aldehydes or carboxylic acids used in some other methods of ester synthesis.
- **Catalysis:** The reaction typically involves using transition metal catalysts, which can be efficient and reused, making the process more sustainable.

The catalysts employed in these reactions constitute another focal point for green chemistry research. Although many effective catalysts are derived from precious metals such as ruthenium or iridium, there is a concerted effort to develop catalysts based on more abundant and less costly metals like iron or nickel. This transition addresses concerns of resource scarcity and mitigates the environmental impact associated with the extraction and processing of rare metals.

Moreover, the concept of acceptorless dehydrogenative coupling transcends mere ester synthesis. The same principles can be employed in the synthesis of other significant organic compounds, including amides, imines, and even polymers. This versatility renders the method particularly appealing from an industrial standpoint, as it has the potential to streamline multiple production processes under a unified, more environmentally friendly methodology.

It is crucial to acknowledge that despite the substantial advantages this method offers, it also encounters challenges in achieving widespread adoption. Catalytic systems frequently require optimization for specific substrates.

The transition towards more sustainable methods of ester production, as demonstrated by techniques such as acceptorless dehydrogenative coupling, marks a substantial advancement in the realm of sustainable chemistry. By concurrently addressing multiple tenets of green chemistry – including atom economy, waste minimization, safer processes, and the generation of valuable byproducts – these novel methodologies are setting the stage for a more environmentally conscious chemical industry. As research continues and these methods are refined and scaled up, they hold the promise of revolutionizing not only ester synthesis but a broad spectrum of chemical processes, thereby contributing to a more sustainable future for the chemical industry and beyond.

1.2 Previous Earth-Abundant Metal Catalyst: Past Ligand Structures in the Conversion of Primary Alcohols to Esters

Tetradentate tripodal ligands are chelating agents that are widely employed in coordination chemistry and catalysis. These ligands are defined by their structural conformation, which coordinates them with metal centers via four donor atoms. In the case of these ligands, three

electoral donor groups are linked to the central atom, which can be nitrogen or carbon, and the fourth is connected to any of the groups of the 'ears' of a tripod.

They are compatible with a broad range of transition metals, from first-row elements, including iron and cobalt, to second and third-row elements, which incorporate rhodium and iridium, respectively, into the metal center of the resulting complex. This wide-ranging compatibility has seen them widely used in homogeneous catalysis, significantly when small molecules are activated and transformed.

Recent studies have looked into these ligands' effectiveness in various catalytic reactions. Our group previously synthesized and designed a new tetradentate tripodal ligand, $^{ipr}PPPN^{H}Py^{Me}$, with MLC (metal-ligand cooperativity) based on an N-H linker between the pyridine ring and the phosphine moiety.[20] It was illustrated that an air-stable complex of cobalt, identified as 1a (Scheme 1.2), with this new ligand could catalyze the dehydrogenation of secondary alcohols to ketones.

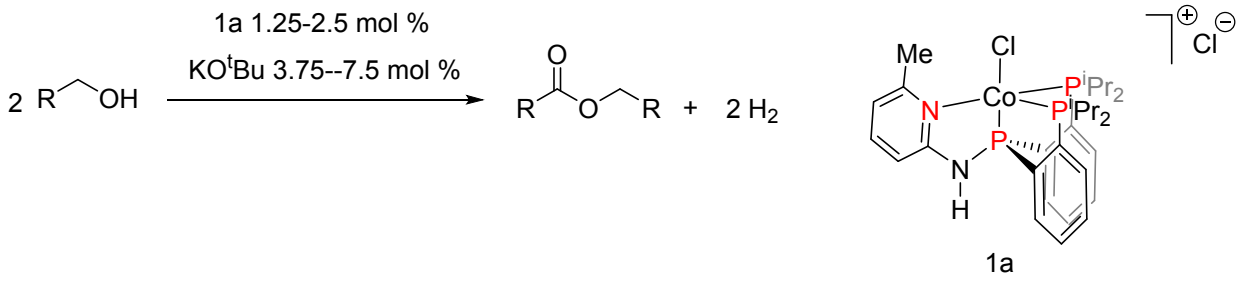

Scheme 1.2 KO^{t}Bu-Catalyzed Dehydrogenative Coupling of Primary Alcohols[20]

Based on these discoveries, further studies were directed at the development of the usage area of this catalytic system. Here, we report that a straightforward reaction of complex 1a with potassium

tert-butoxide (KO^tBu) enables the acceptorless dehydrogenative homocoupling of primary alcohols to esters. This work marks valuable progress in the catalytic alcohol transformation field, which proves the applicability of the newly designed ligand in a plethora of organic reactions.

The catalytic system was compatible with various substrates and could engage aromatic and aliphatic primary alcohols. This reaction demonstrated substituent and electronic group independence to aryl rings of the substrate, including electron donor and acceptor groups. Of particular interest was that the system also effectively converted diol to lactone transformation.

Mechanistic studies gave an understanding of the reaction pathway and its functions in the catalytic system of varied species. Notably, the N-H linker in the ligand did not significantly impact the mentioned transformation. The base, KO^tBu, was used for catalyst activation and to facilitate a Tishchenko-type pathway. A reasonable reaction mechanism was suggested: the Co-catalyzed dehydrogenation of alcohol to aldehyde and the following Tishchenko pathway with base participation.

This work demonstrated for the first time that base transition metal complexes supported by a tetradentate tripodal ligand could effectively facilitate this transformation. The catalyst was evaluated and found to be homogeneous through a mercury poisoning test, while hydrogen gas was observed to be given off as a byproduct in the process.

The system's efficiency was illustrated by high yields in many substrates, with some exceeding 90% under optimal conditions. It also demonstrated an elevated level of atom economy because the only other product formed, besides the desired products, is hydrogen gas. This work is highly beneficial in expanding the field of green catalysis through synthesizing esters from alcohols with

the help of an earth-abundant transition metal, cobalt. The findings of this work laid the foundation for an evolution of the base metal catalysts that could be used in conversions of a similar nature, hence the possible replacement of precious metal catalysts to achieve sustainable solutions.

1.2.1 Works by Other Research Groups

Jones and colleagues created a unique catalyst system based on nickel to facilitate the dehydrogenative coupling of benzyl alcohol into benzyl benzoate.[7] The catalyst, designated Tp'Ni(QR), is based on the combination of a quinolinate (Q) ligand with H, Me, CF_3 substituents (R) and a tris(3,5-dimethylpyrazolyl)borate (Tp') ligand.

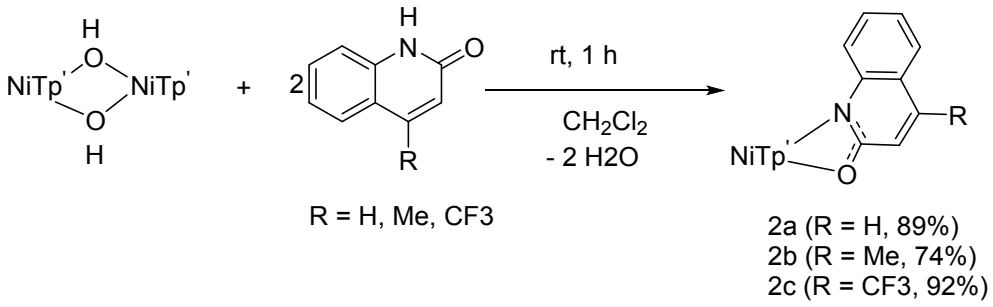

Scheme 1.3 Synthesis and X-ray Structures of Tp′Ni(Q^R) Complexes[7]

Out of all the series evaluated, the catalyst Tp'Ni(QCF_3) was the most effective. When benzyl alcohol was used as the substrate, benzyl benzoate was produced under optimized circumstances (5 mol% catalyst, refluxing toluene, 24 hours). This outcome is reported in Table 1, entry 11 of the study.

Significantly, the absence of benzaldehyde from the reaction mixture suggests that the catalyst favors the dehydrogenative coupling pathway over simple aldehyde dehydrogenation. This selectivity is significant because it shows that the catalyst can enable a more complicated reaction.

The 2-hydroxyquinoline ligand, according to the authors, is essential to the catalytic cycle. Simple Tp'Ni precursors devoid of this ligand in control tests had deficient catalytic activity, emphasizing the critical role played by the quinolinate ligand in facilitating the dehydrogenative coupling process.

In a separate study, Bernskoetter, Hazari, Holthausen, and associates substantially improved the dehydrogenation of methanol to methyl formate in a different work.[8] Their research focused on an iron complex that a PNP pincer ligand stabilized.

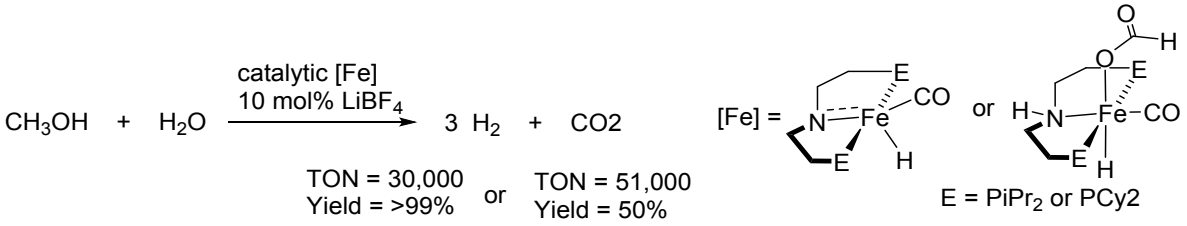

Scheme 1.4 Methanol Dehydrogenation[8]

Utilizing iron, a transition metal widely available on Earth, is consistent with the increased focus on creating sustainable catalytic systems. Since iron is the fourth most plentiful element in the crust of Earth, it is a desirable substitute for the precious metals typically used in catalysis due to its relatively low toxicity.

More recently, Gauvin and colleagues showed the value of a manganese-based catalyst for dehydrogenating primary alcohols to esters that also included a PNP pincer ligand.[9]

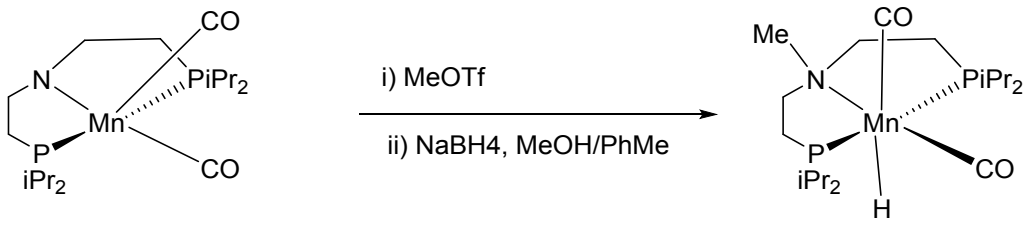

Scheme 1.5 Synthesis of [Mn(H)(CO)$_2$(*Me*PNP)][9]

This work expands the scope of base metal catalysts capable of performing such transformations. Manganese, like iron, is an abundant and cost-effective metal, making it an attractive option for large-scale applications. The success of the Mn-PNP system in catalyzing the dehydrogenation of primary alcohols suggests a broad substrate scope, potentially opening avenues for the synthesis of a wide range of ester products.

These three studies collectively highlight several important trends in the field of catalytic alcohol dehydrogenation:

1. Shift to earth-abundant metal catalysts
2. Advanced ligand design
3. Focus on hydrogen production as a valuable by-product
4. Development of atom-economical processes (direct alcohol to ester conversion)

1.3 Pincer Ligand Design for Dehydrogenative Coupling of Primary Alcohols

1.3.1 Pincer Ligands

Pincer ligands have emerged as a superior class of tridentate ligands in organometallic chemistry and homogeneous catalysis during the past decades. Initially described in the late 70's by van

Koten and Shaw,[10,11] pincer ligands function as tridentate chelating species that bind to metal centers in a meridional fashion to generate two fused metallacycles.[12] The most common geometrical arrangement for the ligands is a central donor ligand coordinated to two side donor ligands; this arrangement is usually summarized as ECE, where E stands for a side donor atom, and C stands for the donor at the center.

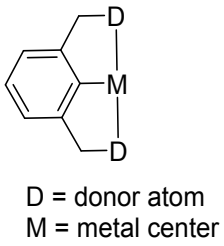

Figure 1.1 Pincer Ligand Arrangement

One significant advantage of the pincer ligands is the possibility of fine-tuning the size and electronic effect depending on modifications of the donor atom, the linking group, or the substituents.[12] This character constitutes a mode of rational design of metal complexes with desired reactivity. On the same note, the chelate effect is strong through tridentate binding mode, and intersperses thermal stability on pincer complexes as they are used in harsh reactions.[13]

Depending on the characteristics, pincer ligands can be divided into palindromic and nonpalindromic pincer ligands and charged and neutral pincer ligands.[12] Popular neutral palindromic pincers are of PCP, PNP, and NCN types, and monoanionic pincers like PCP- . The central donor is usually an aryl or pyridine group, which would prove weak if used as a monodentate ligand but is secure in the pincer complex.[12]

It is worth emphasizing that many pincer complexes can stabilize such exotic targets as non-standard metal oxidation states and coordination geometries.[12,14] For instance, van Koten and coworkers described air-stable divalent Ni(III) complexes coordinated by NCN pincer ligands due to steric shielding provided by NMe_2 groups.[10]

In most pincers, the tridentate coordination mode is rigid and must maintain meridional geometry, but few flexible designs may coordinate in the facial mode.[12] This geometric control is beneficial in catalytic applications since it offers the possibility of accurately positioning ancillary ligands. The limited rotation of donor groups in many pincers also gives well-defined steric environments, a suitable technique for asymmetric catalysis.[15]

Pincer complexes have been extensively utilized as homogeneous catalysts in various transformations.[13,16] Their thermal stability allows for high-temperature operation, while their modular ligand design enables fine-tuning. [12] Additionally, the rigid structures of pincer complexes make them well-suited for anchoring on solid supports, facilitating the development of reusable heterogeneous catalysts.[12]

Pincer chemistry was initially concerned with late transition metals, but lately, it has been successfully generalized to main group elements and early transition metals.[12] New electron donors other than C, N, and P are also under investigation; lewis acid such as boron are being considered. These have been helping to open new directions in catalysis and small molecule activation.

1.3.2 ^{iPr}PPPBF Ligand: A Multifaceted Stabilizer

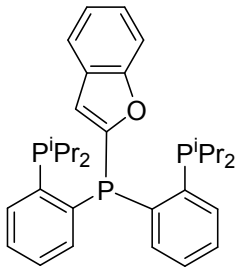

Figure 1.2: The proposed ^{iPr}PPPBF Ligand

The ^{iPr}PPPBF pincer ligand presented in this work offers several advantages in catalytic systems, due to its versatility, which significantly contributes to the stability, reactivity, and selectivity of these complexes.[12,18]

1. **L-Type Ligand Characteristics**: The ^{iPr}PPPBF is an L-type ligand, meaning it donates an electron pair without changing the metal's oxidation state. This characteristic is central to its catalytic role:

Electron Donation: The ligand donates both electrons in the metal-ligand bond, preserving the metal ion's valency, which is crucial for maintaining catalytic activity and enhancing the metal center's stability.

Coordination Flexibility: The ligand's ability to form single bonds without affecting the metal's oxidation state provides a flexible coordination sphere, suitable for multistep reaction sequences and redox transformations.

2. **Phosphine Ligand Properties**: The presence of phosphine in its structure classifies ^{iPr}PPPBF as an ancillary ligand, greatly enhancing the final metal coordination stability:

Chemical Stability: Phosphine ligands do not undergo chemical changes during reactions, making them essential for formulating solid, stable catalysts capable of withstanding demanding reaction conditions.

Supportive Role: As ancillary ligands, phosphines support the reaction cycle by stabilizing the complex structure during catalysis, thereby increasing efficiency.

3. **Electronic Properties**: Strong σ-donor and weak π-acceptor characteristics contribute to the ligand's effectiveness:

Back-Bonding: A combination of strong σ-donation and weak π-acceptance enables back-bonding, where electron density flows from the metal to the ligand's vacant orbitals.

Bond Strengthening: Back-bonding reduces the metal-ligand distance, strengthening the bond and improving the overall stability of the complex, protecting it from decomposition during reactions.

Electronic Fine-Tuning: The balance between σ-donation and π-acceptance allows fine-tuning of the metal center's electronic structure, optimizing catalytic properties for specific reactions.

4. **Pincer Ligand Architecture**: The ^{iPr}PPPBF ligand belongs to the pincer ligand family, known for its unique tridentate binding mechanism:

Rigid Structure: Pincer ligands form three rigid connections with the metal center, creating a thermally stable, precise structure that can be tailored for specific catalytic applications.

Predictable Geometry: The fixed spatial arrangement of pincer ligands allows the creation of catalysts with precisely controlled three-dimensional architectures, enhancing selectivity and activity.

5. **Benzofuran Group Contributions**: The inclusion of a benzofuran moiety in the ^{iPr}PPPBF ligand introduces additional functionality:

Electron-Rich Nature: The benzofuran group increases the electron density of the ligand, which may influence the metal center's reactivity.

Hydrogen Bonding: The oxygen atom in the benzofuran ring can participate in hydrogen bonding, stabilizing transition states or intermediates, thereby improving reaction rates and selectivity.

The effects of phosphine ligands in catalysis have been known for some time, dating back to their use in the "Reppe" chemistry involving alkynes, alcohols, and carbon monoxide, where a phosphine-ligated nickel catalyst was more efficient than the unligated catalyst.[17] This intricate design of the ^{iPr}PPPBF ligand enhances both the stability and reactivity of metal complexes, making it a promising candidate for future catalytic applications.

1.3.3. Advantages of Cobalt as a Catalytic Center

The development of inexpensive, less toxic first-row transition metal catalysts has gained considerable momentum as a more environmentally-benign and economically-attractive alternative to the widely used precious 4d or 5d transition metal catalysts.[19] The use of cobalt in

combination with ^{iPr}PPPBF ligand offers several advantages over traditional precious metal catalysts:

Sustainability and Cost-Effectiveness

Abundance: As a first-row transition metal, cobalt is significantly more cost-effective than precious metals like platinum or palladium. Its abundance lowers production costs and enhances the sustainability of catalyst development.

Environmental Impact: Cobalt extraction and processing have a comparatively lower environmental impact than that of precious metals, aligning with green chemistry principles.

Unique Reactivity

Redox Flexibility: Cobalt can exist in various oxidation states, such as Co(I), Co(II), and Co(III), making it highly adaptable in catalytic cycles. This redox flexibility can be exploited to develop new transformations or optimize existing ones.

Spin State Variability: Cobalt's ability to form low-spin, intermediate-spin, and high-spin complexes offers opportunities to manipulate reactivity. Spin states can influence substrate binding, activation, and product release, leading to enhanced selectivity.

Complementarity with ^{iPr}PPPBF

Electronic Tuning: The strong σ-donor character of the ^{iPr}PPPBF ligand increases electron density at the cobalt center, facilitating oxidative addition processes and stabilizing higher oxidation states.

Steric Control: The extended pincer structure of the ^{iPr}PPPBF ligand provides a well-defined steric environment around the cobalt center, allowing for fine-tuned substrate access and binding, which improves selectivity in catalytic reactions.

1.4 **Objective of the study**

The primary purpose of this study is to provide a detailed analysis of the cobalt-catalyzed dehydrogenative coupling reaction and its sustainability as a more environmentally friendly method for ester synthesis. We achieve this goal through the following sub-objectives, which we crafted to support promoting sustainable chemistry practices.

Firstly, it aims to design and enhance a suitable cobalt-based catalytic system for selectively accomplishing the dehydrogenative coupling of primary alcohols. This objective comprises the preparation and stabilization of new cobalt complexes with specific emphasis on modifying ligands to raise the catalysts' efficiency, selectivity, and stability. We will optimize coupling reaction by a systematic alteration of some reaction conditions, including temperature, the choice of solvent, and the amount of catalyst. We will perform catalytic analysis to determine the slow step of the reaction and the order of the reaction concerning the components. In situ, we will also use NMR spectroscopy to ascertain reaction intermediates.

Another purpose of our work is to delineate the potential and constraints of the cobalt-catalyzed dehydrogenative coupling reaction. Besides, to consider the method more general, we want to explore primary alcohol substrates with diverse types of groups. These will comprise aliphatic, aromatic, and functionalized primary alcohols to determine the compatibility of the catalytic system with several functional groups. By changing the structural properties of the alcohol

substrates in a controlled manner, we aim to learn structure-activity relations that would help in the further application of this approach. Following the principles of green chemistry, we hope to explore the feasibility of using renewable substrates. This entails understanding the reactivity of primary alcohols to make esters obtained through biorenewable feedstocks.

An important consideration of our research aims, and scope is assessing the green chemistry perspective of the cobalt-catalyzed dehydrogenative coupling strategy. Our main objective is to evaluate the sustainability of the reaction's efficiency using principles such as atom economy, energy, and waste. We also hope to evaluate the possibility of recycling and reusing the cobalt catalyst, which is vital for the long-term sustainability of the process. Also, we will look into the possibility of capturing and using the hydrogen gas produced in the process; others may incorporate the idea into other chemical processes or energy-producing mechanisms.

An additional objective of our study is to assess our newly developed cobalt-based catalytic system against other transition metal complexes employed in analogous transformations. Hence, we will base this comparative analysis on activity, selectivity, and other factors, including the cost and availability of the metal catalysts and their impact on the environment. Thus, this comparison aims to attempt to define whether cobalt catalysis has any distinct advantages and shortcomings when applied to dehydrogenative coupling reactions.

Finally, another aim of the present work is to advance the scientific knowledge of the cobalt-catalyzed processes and dehydrogenative coupling transformations. The realizations of the detailed mechanistic investigations and the substrate scope studies will help us understand the reactivity of the cobalt complexes and the factors that can control alcohol dehydrogenation and

coupling pathways. As such, these insights could expand to other related transformations and the ability to apply our research findings to forming new catalytic systems.

CHAPTER 2

EXPERIMENTAL METHODOLOGY

2.1. General Methods

Unless otherwise is stated, all reactions were set up in an MBraun glovebox under an atmosphere of N_2 and standard air-free techniques were used to carry out reactions. The solvent was dried by passing through a Pure Solv solvent purification system installed with activated alumina columns. Organic substrates were purchased from Oakwood Chemical, Fisher Scientific, and Sigma Aldrich. Substrates with in-tact SURE/SEAL were used directly, and substrates without air-free seals were dried with molecular sieves (4 Å) before use. Bases such as KO^{t}Bu, NaO^{t}Bu, and NaOMe were vacuum sublimed before use. Buchi Rotavapor R-200 was used to remove the solvent from samples during work-up. JEOL Unity 500 MHz or 300 MHz spectrometer were used to record NMR spectra. Trimethylsilane (0.00 ppm) was used as a reference in C_6D_6 and $CDCl_3$ to record ^{1}H NMR spectra. The NMR spectra for the known compounds are comparable with the previously reported ones.

2.2 Experimental Methods

2.2.1 Synthesis of ^{iPr}PPPBF Ligand

The synthetic pathway for the ^{iPr}PPPBF ligand was refined to improve efficiency. A fundamental discovery was that the order of reagent addition could be modified: n-butyllithium (^{n}BuLi) could be introduced to benzofuran first (step 3), followed by adding the product from steps 1-2. This approach proved more straightforward than adding the product from steps 1-2 to benzofuran before introducing ^{n}BuLi.

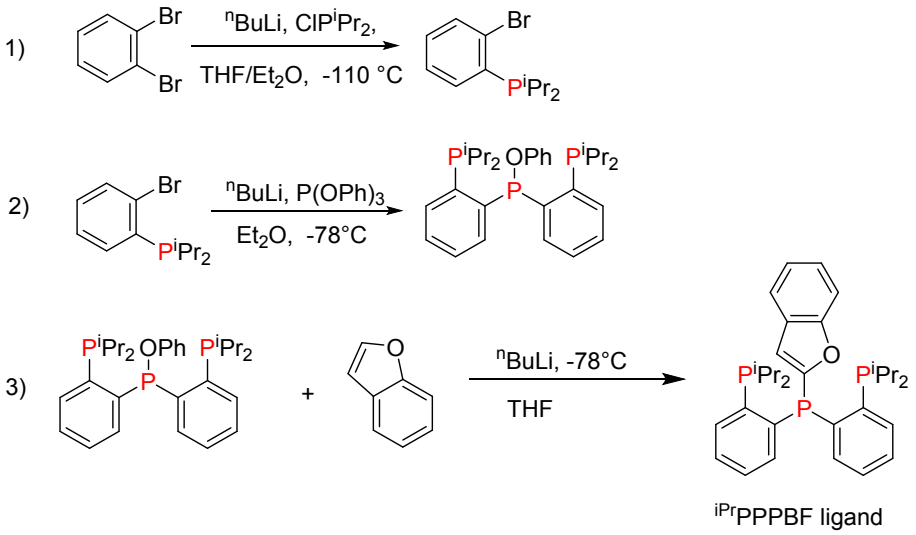

Scheme 2.1 Synthesis of ^{iPr}PPPBF Ligand

The synthesis was handled in the cold well inside the glovebox. It begins with preparing two separate reaction mixtures in Erlenmeyer flasks: Flask A and Flask B.

For Flask A, 2 grams of 1-bromo-2-diisopropylphosphorobenzene are combined with 12 mL of tetrahydrofuran (THF) in a 250 mL Erlenmeyer flask. This mixture is cooled to -78°C and stirred for 25 minutes. Then, 4.66 mL of n-butyllithium (1.6 M in hexane) is added dropwise at -78°C, causing the solution to turn yellow immediately. The reaction mixture continues stirring at -78°C for 1 hour, during which it remains yellow but becomes cloudy.

In a separate vial, 1.136 g of triphenylphosphite is dissolved in 12 mL of THF and cooled to -78°C for 15 minutes. This solution is then added dropwise to Flask A at -78°C, resulting in an orange, clear reaction mixture. The contents of Flask A are stirred at -78°C for 1.5 hours, followed by 1 hour at room temperature, with no observed color change.

Simultaneously, Flask B is prepared by combining 1.297 g of benzofuran with 40 mL of THF in another 250 mL Erlenmeyer flask. This solution is cooled to -78°C and stirred for 15 minutes. Subsequently, 6.86 mL of n-butyllithium (1.6 M in hexane) is added dropwise at -78°C. The solution initially turns clear yellow during this addition, gradually becoming yellow and cloudy. This mixture is stirred for 1 hour.

Meanwhile, Flask A is cooled again to -78°C at least for 15 minutes for the final steps. The contents of Flask A are then added dropwise to Flask B at -78°C, initially forming a cloudy orange solution. The combined reaction mixture is allowed to warm to room temperature while stirring for 12 hours, during which the solution becomes clear orange.

A ^{31}P NMR analysis is performed to confirm the desired product's formation. The stability of the product is verified by exposing a sample to air for 7 days and conducting another ^{31}P NMR, which proves that the product remains stable.

2.2.2 Purification Process

The synthesized ligand is removed from the nitrogen environment and exposed to atmospheric conditions. The addition of deionized water neutralizes excess n-butyllithium. The reaction solvent, THF, is then removed using a Buchi R-210 rotary evaporator.

The resulting mixture undergoes a series of three extractions using dichloromethane (DCM). The combined organic fractions are washed with brine to remove any remaining impurities. These organic layers are then dried over magnesium sulfate for 15 minutes.

The organic solution is filtered through a Hirsch funnel equipped with a celite pad to separate the drying agent. The filtrate is then concentrated using the rotary evaporator to remove the DCM, yielding a sticky yellow oil. The oil is redissolved in a small volume of DCM for crystallization and transferred to a vial. A layer of methanol is carefully added on top of the DCM solution. The vial is then refrigerated for crystallization, which takes approximately three days. After the initial crystallization, the supernatant liquid is carefully removed by pipette. The resulting yellow-tinted crystals are redissolved in DCM, and the methanol layering process is repeated. This recrystallization yields colorless crystals. The purity of the crystal is confirmed by NMR (^{1}H, ^{13}C and ^{31}P) analysis.

2.2.3 Structure Characterization

Small amount of colorless crystals were dissolved in CD_2Cl_2 for NMR analysis. NMR spectra were recorded on a JEOL Unity 500 or 300 MHz spectrometer. ^{1}H NMR spectra were referenced to tetramethyl silane (0.00 ppm). ^{13}C NMR were referenced to solvent carbons at 54.2 ppm for CD_2Cl_2. ^{31}P NMR were referenced to 85% H_3PO_4 (0.0 ppm). HRMS were acquired from the Mass Spectrometry and Proteomics Facility at University of Notre Dame.

Mass Spectrometry & Proteomics Facility

Mass Spectrum SmartFormula Report

Analysis Info

Analysis Name	D:\Data\0919\KD1037.d	Acquisition Date	9/19/2023 11:24:27 AM
Method	0911 tune low.m	Operator	BDAL@DE
Sample Name	KD1037	Instrument / Ser#	micrOTOF II 8213750.10314
Comment	direct infusion		

Acquisition Parameter

Source Type	ESI	Ion Polarity	Positive	Set Nebulizer	0.4 Bar
Focus	Not active	Set Capillary	4500 V	Set Dry Heater	180 °C
Scan Begin	50 m/z	Set End Plate Offset	-500 V	Set Dry Gas	4.0 l/min
Scan End	1650 m/z	n/a	n/a	Set Divert Valve	Waste

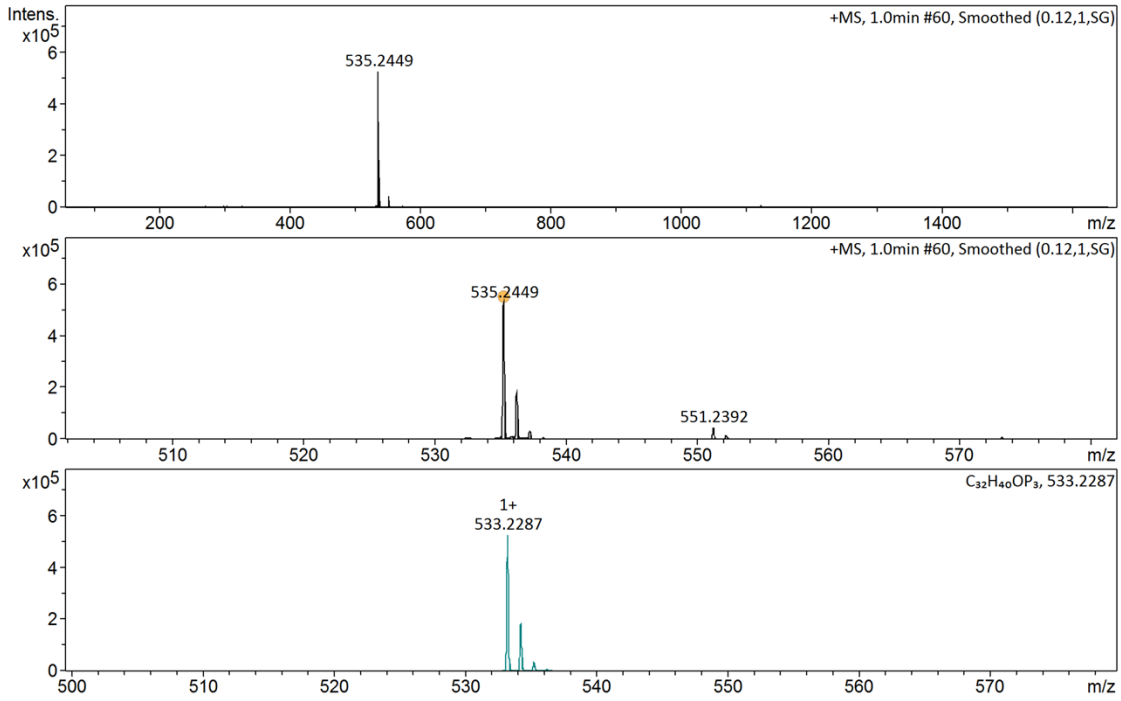

Meas. m/z	#	Ion Formula	m/z	err [ppm]	Mean err [ppm]	rdb	N-Rule	e⁻ Conf
535.244853	1	C32H42OP3	535.244302	-1.0	-0.2	13.5	ok	even

Figure 2.1 HRMS of of ^{iPr}PPPBF Ligand

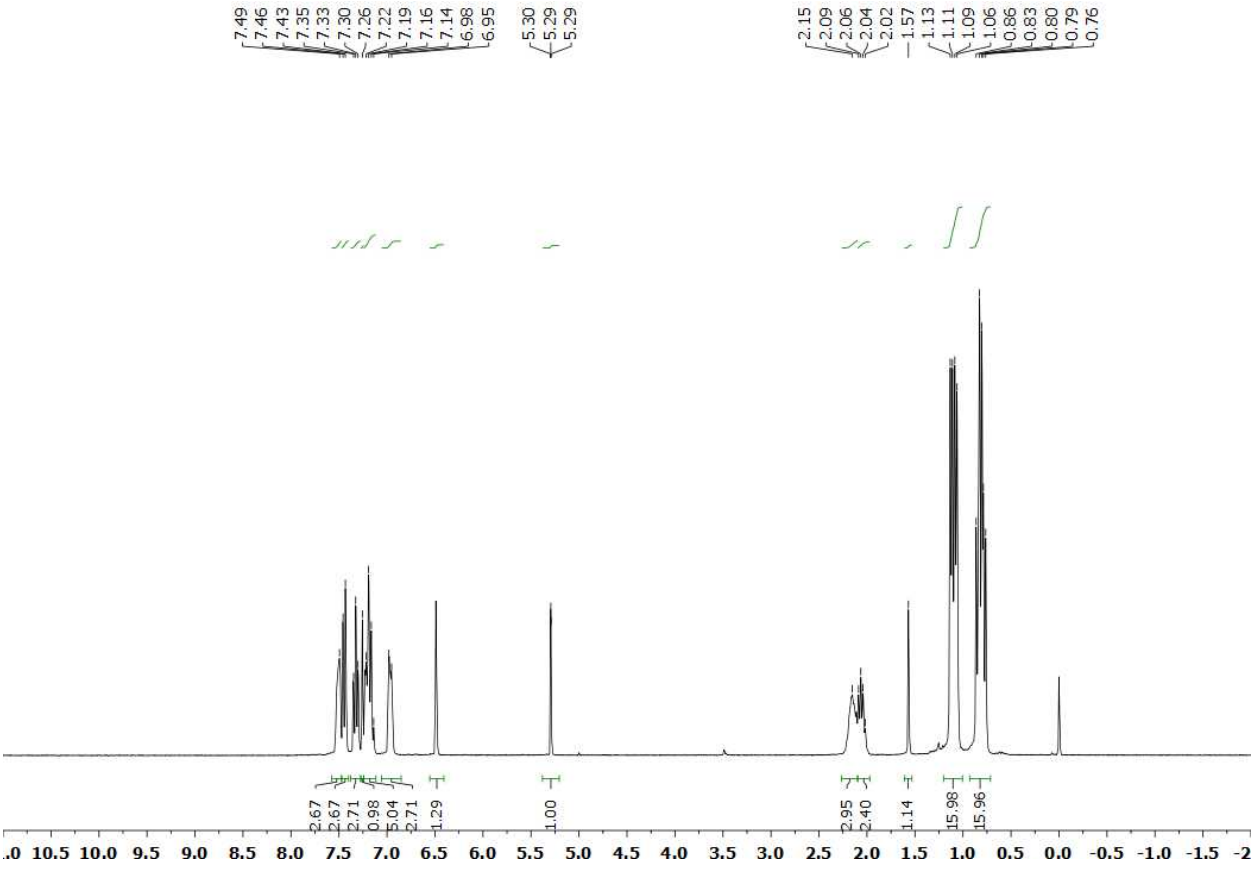

Figure 2.2 ^{1}H NMR spectra (500 MHz) of ^{iPr}PPPBF Ligand in CD_2Cl_2

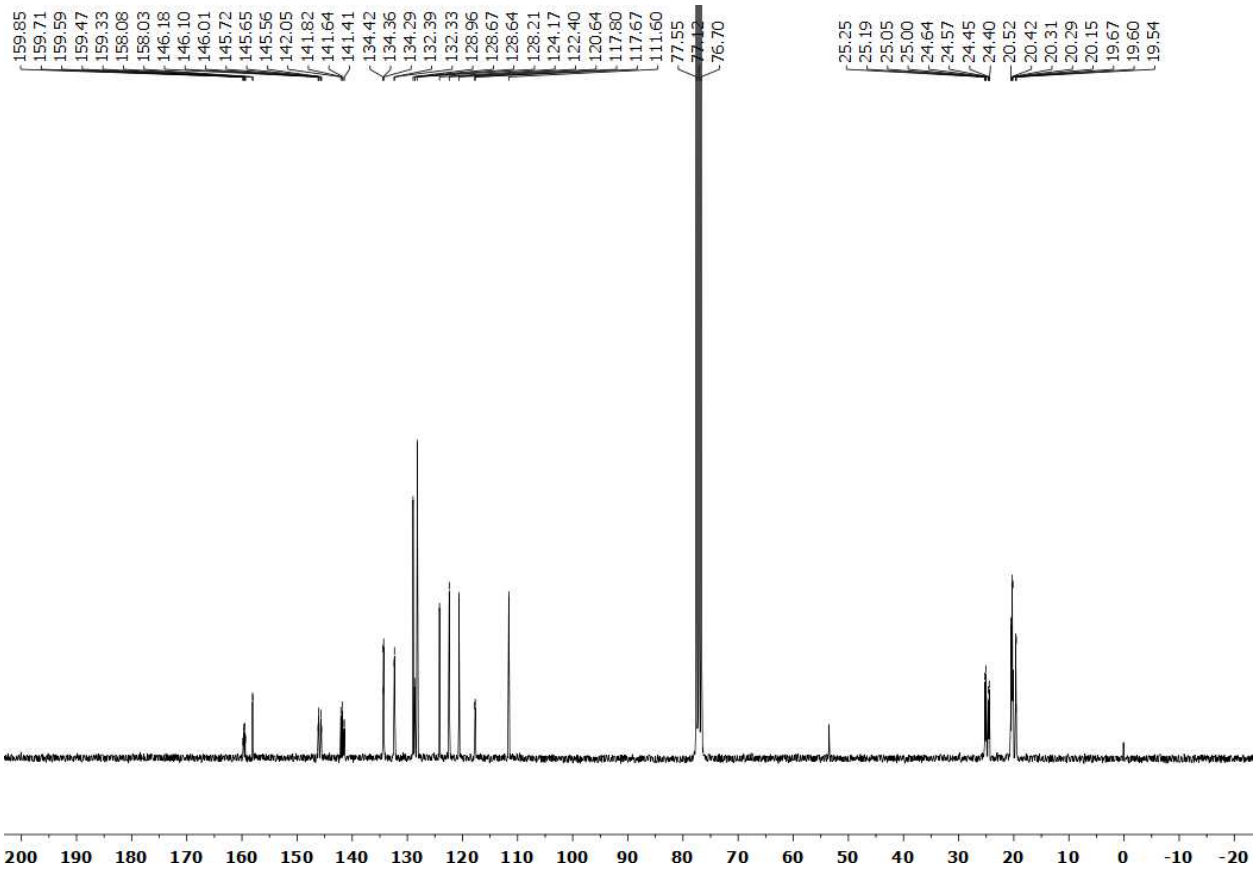

Figure 2.3 $^{13}C\{^{1}H\}$ NMR Spectra (126 MHz) of ^{iPr}PPPBF Ligand in CD_2Cl_2

2.2.4 Synthesis of (^{iPr}PPPBF)$CoCl_2$ complex

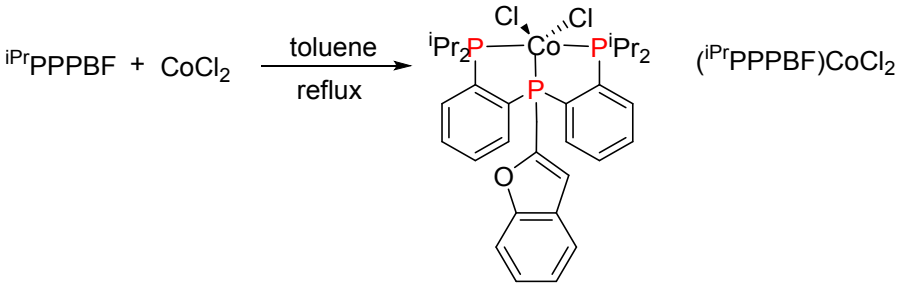

Scheme 2.2 Synthesis of (^{iPr}PPPBF)$CoCl_2$ Complex

The coordination of the ^{iPr}PPPBF ligand with cobalt was initially carried out at room temperature using dichloromethane (DCM) as the solvent. In this process, 25.5 mg of solid, anhydrous cobalt(II) chloride and 100 mg of purified ^{iPr}PPPBF ligand crystals were weighed into separate vials, each containing 2 mL of DCM. To the blue slurry of the cobalt(II) chloride was added the ligand solution dropwise at room temperature. Throughout the addition, the reaction mixture underwent a series of color changes. It remained light blue for most of the process before transitioning to pink and finally reaching a deep red as the reaction progressed. The mixture continued to stir for approximately 48 hours, resulting to a deep red homogeneous solution. Upon completion, the product was stored in a refrigerated, inert atmosphere.

To expedite the coordination process, an alternative approach was explored using toluene as the solvent. This reaction was conducted in an airtight vial filled with a nitrogen atmosphere. The sealed container was removed from the inert environment and heated in an oil bath at 120°C with constant stirring.

Initially, the ligand and cobalt salt exhibited poor solubility in toluene, resulting in a blackish-gray mixture. Despite this, the reaction was allowed to proceed over an extended weekend period. Although the initial appearance was unpromising, the mixture eventually achieved the anticipated deep red color homogeneous solution, indicating successful coordination.

2.2.5 Purification / Crystallization Process

The toluene-based reaction product was divided for further analysis. Half of the sample was removed from the inert atmosphere to assess its air sensitivity. Various solubility tests were conducted on this portion. However, within a few days, all exposed samples degraded, as evidenced by color changes to green, pink, and brown in different aliquots.

The DCM-based reaction product was concentrated under vacuum in an inert atmosphere and refrigerated. Despite several days of storage, this sample failed to produce any crystals.

The remaining toluene-based product, which had been kept under inert conditions, was divided into three portions. The toluene was removed entirely from each portion using a vacuum within the inert atmosphere. The resulting solid residues were then redissolved in DCM. Each solution was subjected to a different crystallization attempt by layering methanol, diethyl ether, or tetrahydrofuran (THF).

The sample layered with diethyl ether successfully yielded dark red needle-shaped crystals among these crystallization attempts. A single crystal from this batch was selected for structural determination using X-ray crystallography.

2.2.6 X-ray Crystallographic Data Collection and Refinement of the Structure

Single orange plate-shaped crystals of KD_006 were isolated from DCM/Et_2O. A orange plate-shaped crystal with dimensions 0.82×0.12×0.06 mm3 was mounted on a suitable support. Data were collected using an SuperNova, Dual, Cu at home/near, Pilatus 200K diffractometer operating at T = 100.00(10) K. Data were measured using ω scans of 0.5° per frame for 39.4 s using Mo Kα radiation. The total number of runs and images was based on the strategy calculation from the program CrysAlisPro (Rigaku, V1.171.40.84a, 2020) The maximum resolution that was achieved was Θ = 29.906° (0.71 Å). The diffraction pattern was indexed The total number of runs and images was based on the strategy calculation from the program CrysAlisPro (Rigaku, V1.171.40.84a, 2020) and the unit cell was refined using CrysAlisPro (Rigaku, V1.171.40.84a, 2020) on 7159 reflections, 31% of the observed reflections. Data reduction, scaling and absorption corrections were performed using CrysAlisPro (Rigaku, V1.171.40.84a, 2020). The final completeness is 92.20 % out to 29.906° in Θ. The absorption coefficient μ of this material is 0.873 mm-1 at this wavelength (λ = 0.711Å) and the minimum and maximum transmissions are 0.604 and 1.000. The structure was solved and the space group P-1 (# 2) determined by the ShelXS (Sheldrick, 2008) structure solution program using Direct Methods and refined by Least Squares using version 2018/1 of ShelXL 2018/1 (Sheldrick, 2015). All non-hydrogen atoms were refined anisotropically. Hydrogen atom positions were calculated geometrically and refined using the riding model. Hydrogen atom positions were calculated geometrically and refined using the riding model.

KD_006

Submitted by: **Keying Ding**
Middle Tennessee State University
Solved by: **Oleksandr Hietsoi**
Sample ID: **KD1019**

R_1=22.15%

Crystal Data and Experimental

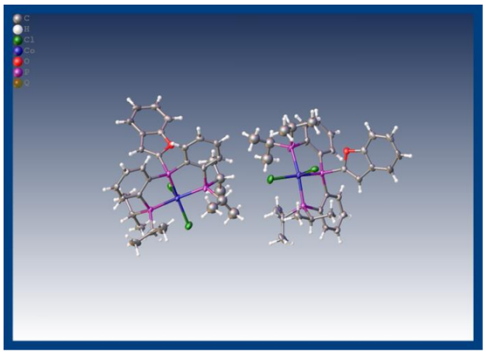

Experimental. Single orange plate-shaped crystals of **KD_006** were isolated from DCM/Et2O. A suitable crystal 0.82×0.12×0.06 mm^3 was selected and mounted on a suitable support on an SuperNova, Dual, Cu at home/near, Pilatus 200K diffractometer. The crystal was kept at a steady T = 100.00(10) K during data collection. The structure was solved with the ShelXS (Sheldrick, 2008) structure solution program using the Direct Methods solution method and by using **Olex2** (Dolomanov et al., 2009) as the graphical interface. The model was refined with version 2018/1 of ShelXL 2018/1 (Sheldrick, 2015) using Least Squares minimisation.

Crystal Data. $C_{64}H_{82}Cl_4Co_2O_2P_6$, M_r = 1328.77, triclinic, P-1 (No. 2), a = 11.2660(5) Å, b = 16.8884(6) Å, c = 17.0433(7) Å, α = 82.753(3)°, β = 89.974(3)°, γ = 89.984(3)°, V = 3216.9(2) Å^3, T = 100.00(10) K, Z = 2, Z' = 1, μ(Mo K$_\alpha$) = 0.873, 22734 reflections measured, 12800 unique (R_{int} = 0.7417) which were used in all calculations. The final wR_2 was 0.2636 (all data) and R_1 was 0.2215 (I > 2(I)).

Compound	**KD_006**
Formula	$C_{64}H_{82}Cl_4Co_2O_2P_6$
$D_{calc.}$/ g cm^{-3}	1.372
μ/mm^{-1}	0.873
Formula Weight	1328.77
Colour	orange
Shape	plate
Size/mm^3	0.82×0.12×0.06
T/K	100.00(10)
Crystal System	triclinic
Space Group	P-1
a/Å	11.2660(5)
b/Å	16.8884(6)
c/Å	17.0433(7)
α/°	82.753(3)
β/°	89.974(3)
γ/°	89.984(3)
V/Å^3	3216.9(2)
Z	2
Z'	1
Wavelength/Å	0.71073
Radiation type	Mo K$_\alpha$
Θ_{min}/°	2.413
Θ_{max}/°	29.906
Measured Refl.	22734
Independent Refl.	12800
Reflections with I > 2(I)	9087
R_{int}	0.7417
Parameters	659
Restraints	0
Largest Peak	2.555
Deepest Hole	-0.940
GooF	0.781
wR_2 (all data)	0.2636
wR_2	0.2327
R_1 (all data)	0.2557
R_1	0.2215

Figure 2.4 X-ray Crystallographic Data for (^{iPr}PPPBF)$CoCl_2$ Complex

2.2.7 High-Resolution Mass Spectrometry (HRMS)

Mass spectrometry (MS) data were acquired on a Bruker micrOTOF II ESI-MS under positive mode.

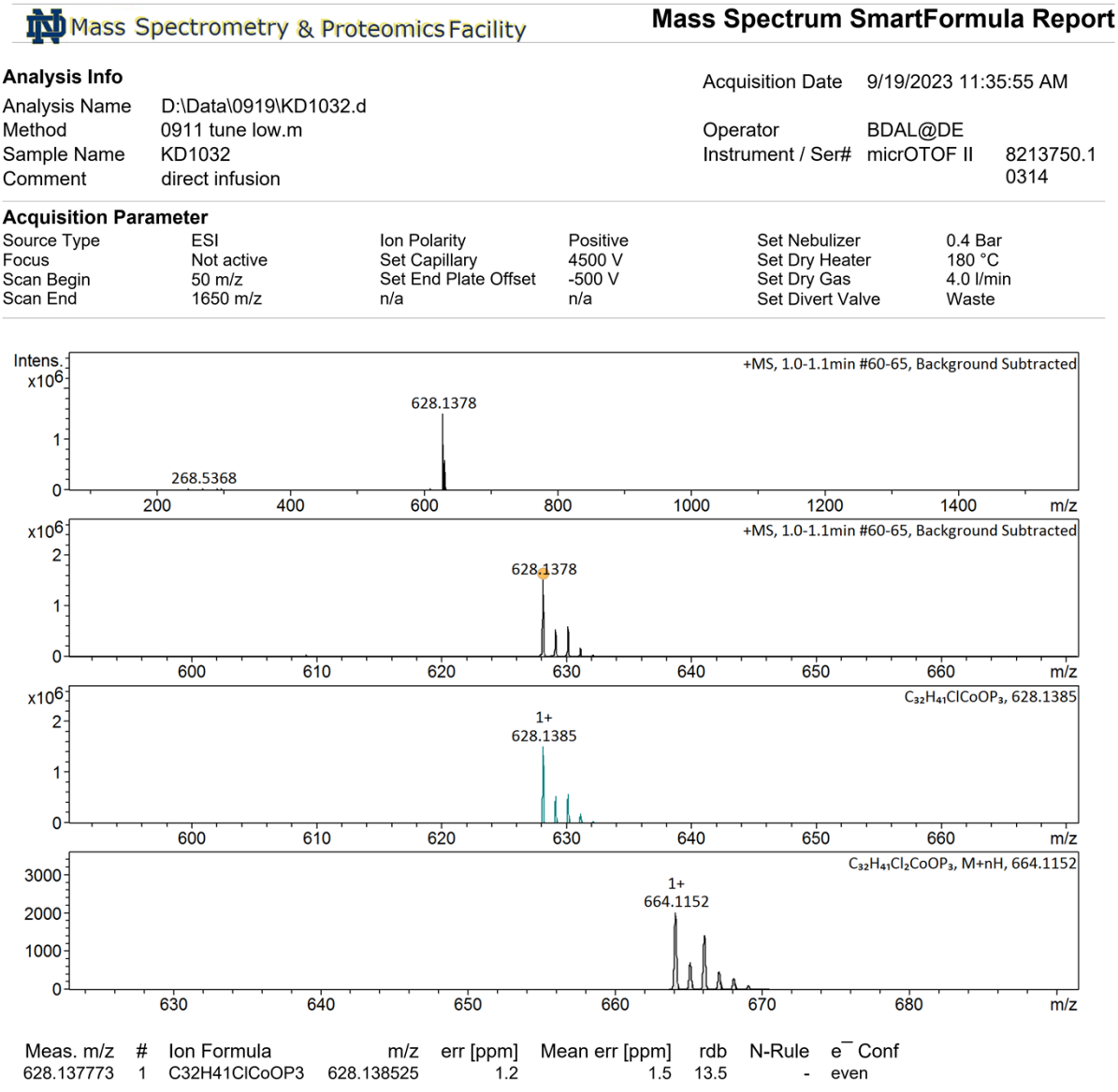

Figure 2.5 HRMS of of (^{iPr}PPPBF)$CoCl_2$ Complex

2.3 Catalytic Studies

2.3.1 Screening of Reaction Conditions on Dehydrogenative Coupling of Benzyl Alcohol

The study on dehydrogenative coupling of benzyl alcohol for ester formation (benzyl benzoate) involves a systematic screening of reaction conditions to optimize the process. This work entails testing various catalyst and additive loadings, and reaction parameters including temperature, solvent, and reaction time. It focuses on achieving high yields and selectivity while minimizing side reactions. The catalyst (^{iPr}PPPBF)$CoCl_2$ is identified as **2a**.

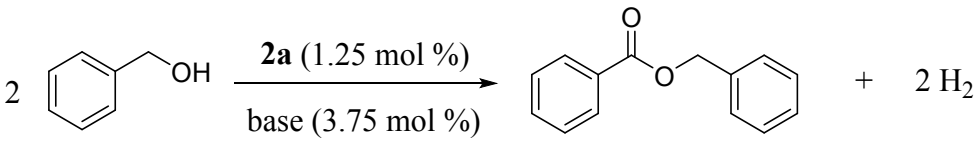

Table 2.1 Optimizations of Reaction Conditions [a,]

Entry	Catalyst	Base	Solvent	Temp (°C)	Yield (%) [b]
1	**2a**	KO^{t}Bu	benzene	80	62
2	**2a**	KO^{t}Bu	benzene	110	78
3	**2a**	KO^{t}Bu	benzene	125	>99, 98[c]
4	**2a**	KO^{t}Bu	toluene	110	61
5	**2a**	KO^{t}Bu	toluene	125	72
6	**2a**	KO^{t}Bu	THF	125	42
7	**2a**	KO^{t}Bu	1,4-dioxane	125	35
8	**2a**	NaO^{t}Bu	benzene	125	95
9	**2a**	NaOMe	benzene	125	82

10	_	KO^{t}Bu	benzene	125	3
11	**2a**	–	benzene	125	0
12	**2a**	KO^{t}Bu	benzene	125	94 [d]

[a] Reaction conditions: **2a** (1.25 mol %), base (3.75 mol %), benzyl alcohol (0.5 mmol), and solvent (0.7 mL) were heated in a sealed 100 mL reaction tube for 24 h. [b] Yields were determined by ^{1}H NMR analysis of the crude reaction mixture with nitromethane as an internal standard. [c] The reaction mixture was heated in a 15 mL reaction tube with an argon balloon on top for 24 h. [d] Mercury (125 mg) was added to the reaction.

2.3.2 Synthetic Details and Characterization Data of Selected Substrates

2.3.2.1 Benzyl Alcohol

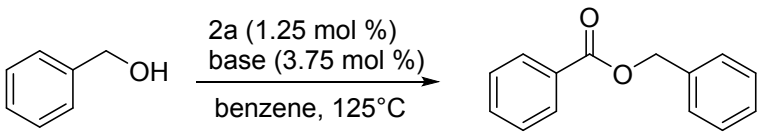

A 15 mL reaction vessel was oven-dried and filled with 2a (4.1 mg, 6.25 μmol, 1.25 mol%), potassium tert-butoxide (2.1 mg, 18.75 μmol, 3.75 mol%), benzyl alcohol (54.1 mg, 0.5 mmol), and benzene (0.7 mL) in a glovebox filled with nitrogen. After sealing the vessel with a screw cap lined with PTFE, the glovebox was opened, and the reaction vessel was brought out of the box. An argon balloon was attached to maintain an inert atmosphere. It was then heated to 125 °C for 24 hours. After the reaction was completed, an internal standard of 8.4 mg 1,3,5-trimethoxybenzene was introduced. Then it was passed through wool and Celite. The resultant mixture was cleaned with deuterated chloroform and put in a tube for an NMR study to be performed on the sample. NMR yield: 97%

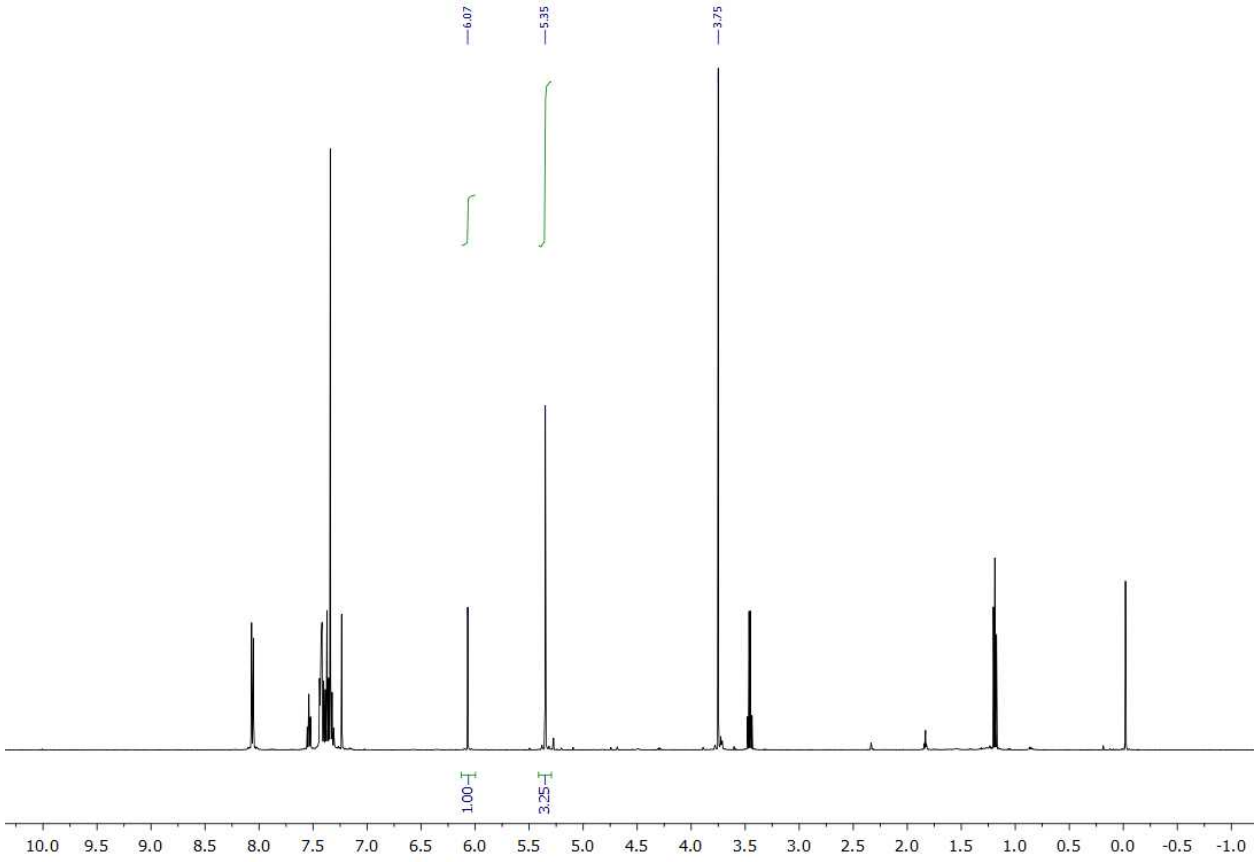

Figure 2.6 ^{1}H NMR (500 MHz, $CDCl_3$) analysis of the reaction mixture from the dehydrogenative coupling of benzyl alcohol

2.3.2.2 4-MethoxyBenzyl Alcohol

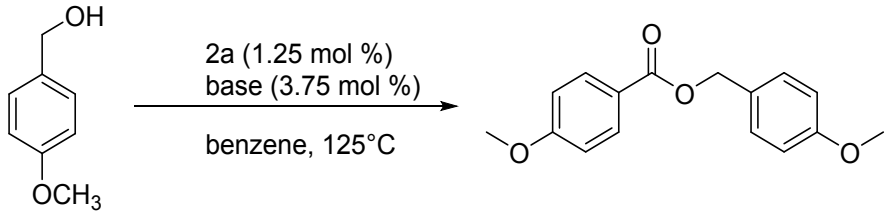

A 15 mL reaction vessel was oven-dried and filled with 2a (4.1 mg, 6.25 μmol, 1.25 mol%), potassium tert-butoxide (2.1 mg, 18.75 μmol, 3.75 mol%), 4-methoxybenzylalcohol (69.1 mg, 0.5 mmol), and benzene (0.7 mL) in a glovebox filled with nitrogen. After sealing the vessel with a screw cap lined with PTFE, the glovebox was opened, and the reaction vessel was brought out of the box. An argon balloon was attached to maintain an inert atmosphere. It was then heated to 125 °C for 24 hours. After the reaction was completed, an internal standard of 1,3,5-trimethoxybenzene (8.4 mg) was added to the mixture. Then it was passed through wool and Celite. The resultant mixture was cleaned with deuterated chloroform and put in a tube for an NMR study to be performed on the sample. NMR yield: 98%

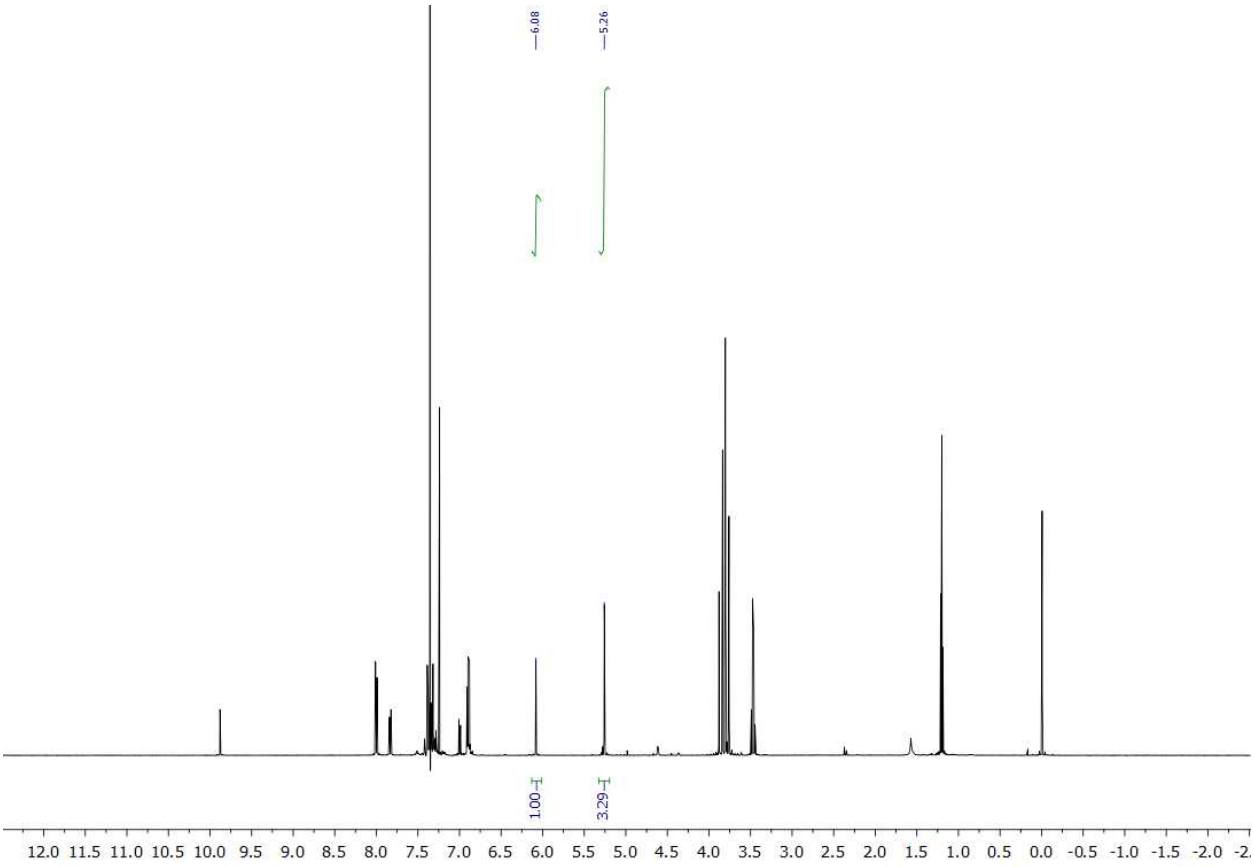

Figure 2.7 ^{1}H NMR (500 MHz, $CDCl_3$) analysis of the reaction mixture from the dehydrogenative coupling of 4-Methoxy benzyl alcohol.

2.3.2.3 4-MethylBenzyl AlcohoL

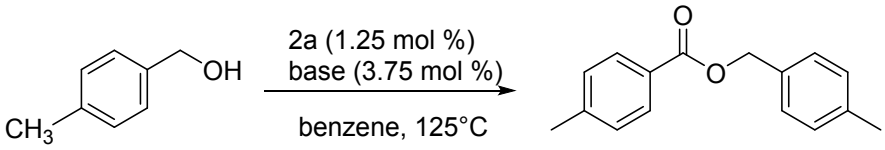

A 15 mL reaction vessel was oven-dried and filled with 2a (4.1 mg, 6.25 µmol, 1.25 mol%), potassium tert-butoxide (2.1 mg, 18.75 µmol, 3.75 mol%), 4-methylbenzyl alcohol (61.1 mg, 0.5 mmol), and benzene (0.7 mL) in a glovebox filled with nitrogen. After sealing the vessel with a screw cap lined with PTFE, the glovebox was opened, and the reaction vessel was brought out of the box. An argon balloon was attached to maintain an inert atmosphere. It was then heated to 125 °C for 24 hours. After the reaction was completed, an internal standard of 1,3,5-trimethoxybenzene (8.4 mg) was added to the mixture. Then it was passed through wool and Celite. The resultant mixture was cleaned with deuterated chloroform and put in a tube for an NMR study to be performed on the sample. NMR yield: 99%

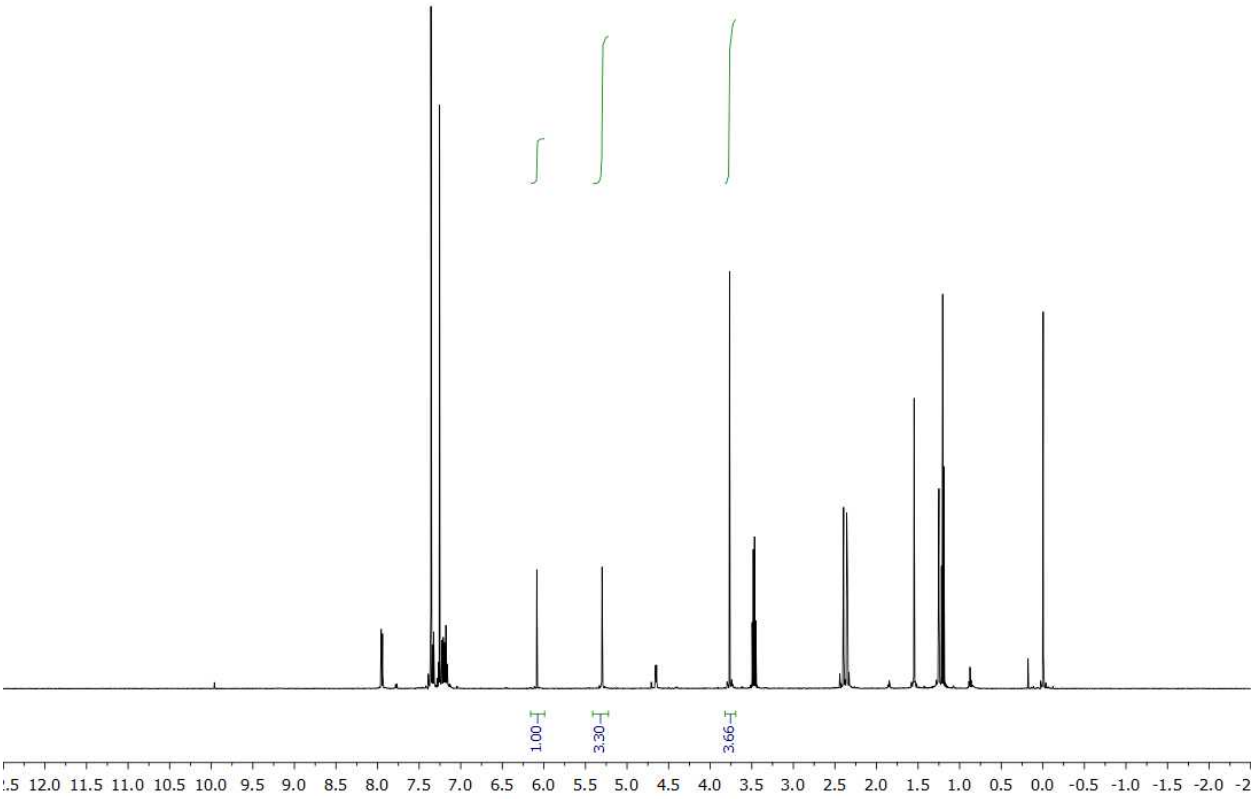

Figure 2.8 ^{1}H NMR (500 MHz, $CDCl_3$) analysis of the reaction mixture from the dehydrogenative coupling of 4-Methyl benzyl alcohol.

2.3.2.4 4-IsopropylBenzyl Alcohol

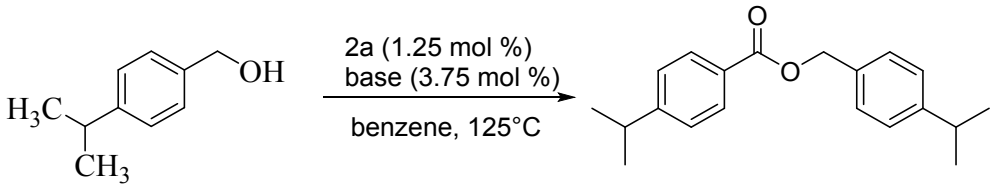

A 15 mL reaction vessel was oven-dried and filled with 2a (4.1 mg, 6.25 μmol, 1.25 mol%), potassium tert-butoxide (2.1 mg, 18.75 μmol, 3.75 mol%), 4-isopropylbenzyl alcohol (75.1 mg, 0.5 mmol), and benzene (0.7 mL) in a glovebox filled with nitrogen. After sealing the vessel with a screw cap lined with PTFE, the glovebox was opened, and the reaction vessel was brought out of the box. An argon balloon was attached to maintain an inert atmosphere. It was then heated to 125 °C for 24 hours. After the reaction was completed, an internal standard of 1,3,5-trimethoxybenzene (8.4 mg) was introduced. Then it was passed through wool and Celite. The resultant mixture was cleaned with deuterated chloroform and put in a tube for an NMR study to be performed on the sample. NMR yield: 94%

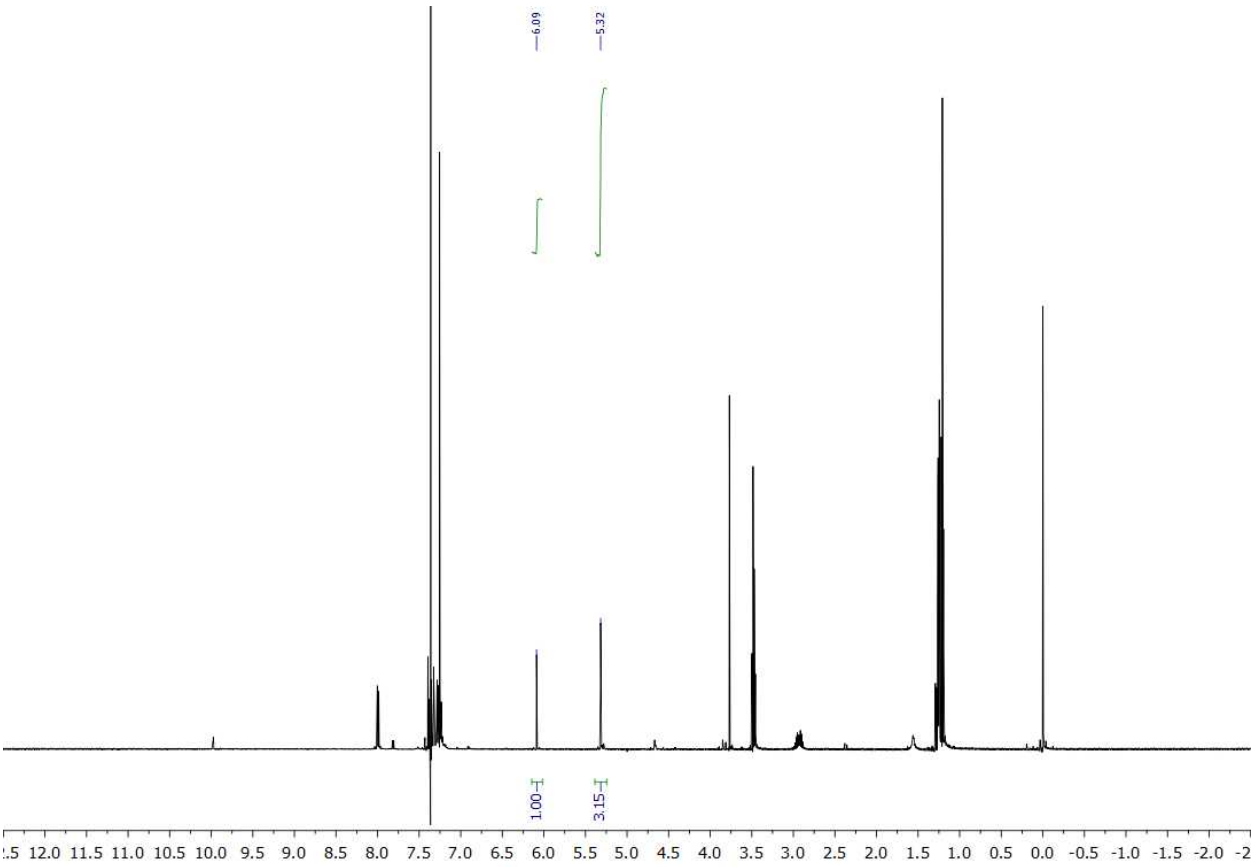

Figure 2.9 ^{1}H NMR (500 MHz, $CDCl_3$) analysis of the reaction mixture from the dehydrogenative coupling of 4-Isopropyl benzyl alcohol.

2.3.2.5 4-ChloroBenzyl Alcohol

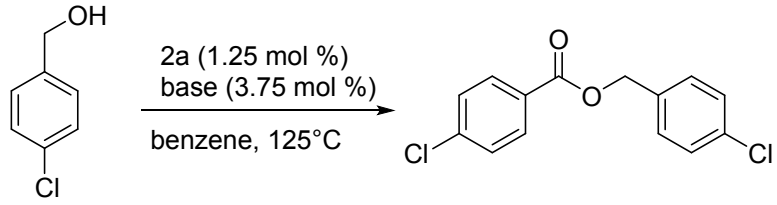

A 15 mL reaction vessel was oven-dried and filled with 2a (4.1 mg, 6.25 μmol, 1.25 mol%), potassium tert-butoxide (2.1 mg, 18.75 μmol, 3.75 mol%), 4-chlorobenzyl alcohol (71.3 mg, 0.5 mmol), and benzene (0.7 mL) in a glovebox filled with nitrogen. After sealing the vessel with a screw cap lined with PTFE, the glovebox was opened, and the reaction vessel was brought out of the box. An argon balloon was attached to maintain an inert atmosphere. It was then heated to 125 °C for 24 hours. After the reaction was completed, an internal standard of 20 μL of nitromethane was introduced. Then it was passed through wool and Celite. The resultant mixture was cleaned with deuterated chloroform and put in a tube for an NMR study to be performed on the sample. NMR yield: 83%

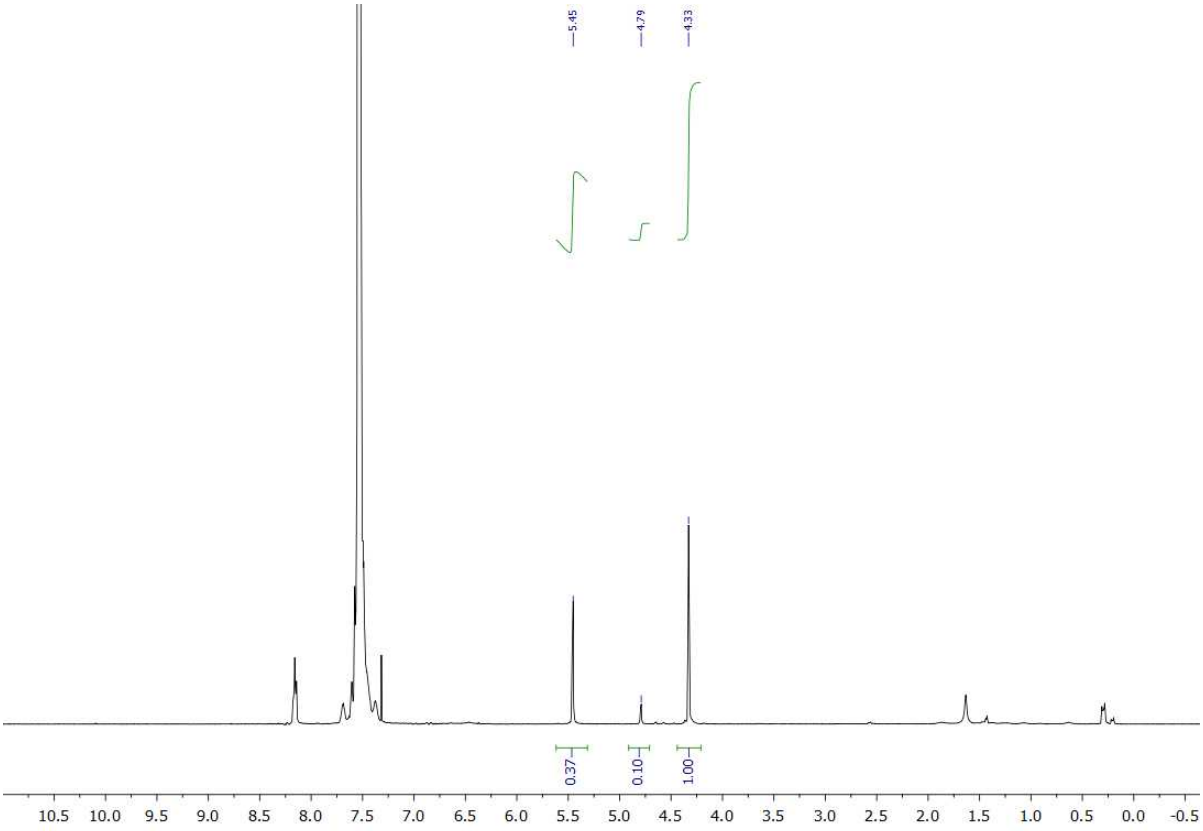

Figure 2.10 ^{1}H NMR (500 MHz, $CDCl_3$) analysis of the reaction mixture from the dehydrogenative coupling of 4-Chloro benzyl alcohol.

2.3.2.6 1-naphthalenemethanol

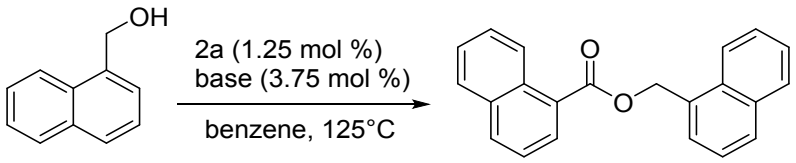

A 15 mL reaction vessel was oven-dried and filled with 2a (4.1 mg, 6.25 μmol, 1.25 mol%), potassium tert-butoxide (2.1 mg, 18.75 μmol, 3.75 mol%), 1-naphthalenemethanol (79.1 mg, 0.5 mmol), and benzene (0.7 mL) in a glovebox filled with nitrogen. After sealing the vessel with a screw cap lined with PTFE, the glovebox was opened, and the reaction vessel was brought out of the box. An argon balloon was attached to maintain an inert atmosphere. It was then heated to 125 °C for 24 hours. After the reaction was completed, an internal standard of 20 μL of nitromethane was introduced. Then it was passed through wool and Celite. The resultant mixture was cleaned with deuterated chloroform and put in a tube for an NMR study to be performed on the sample. NMR yield: 87%

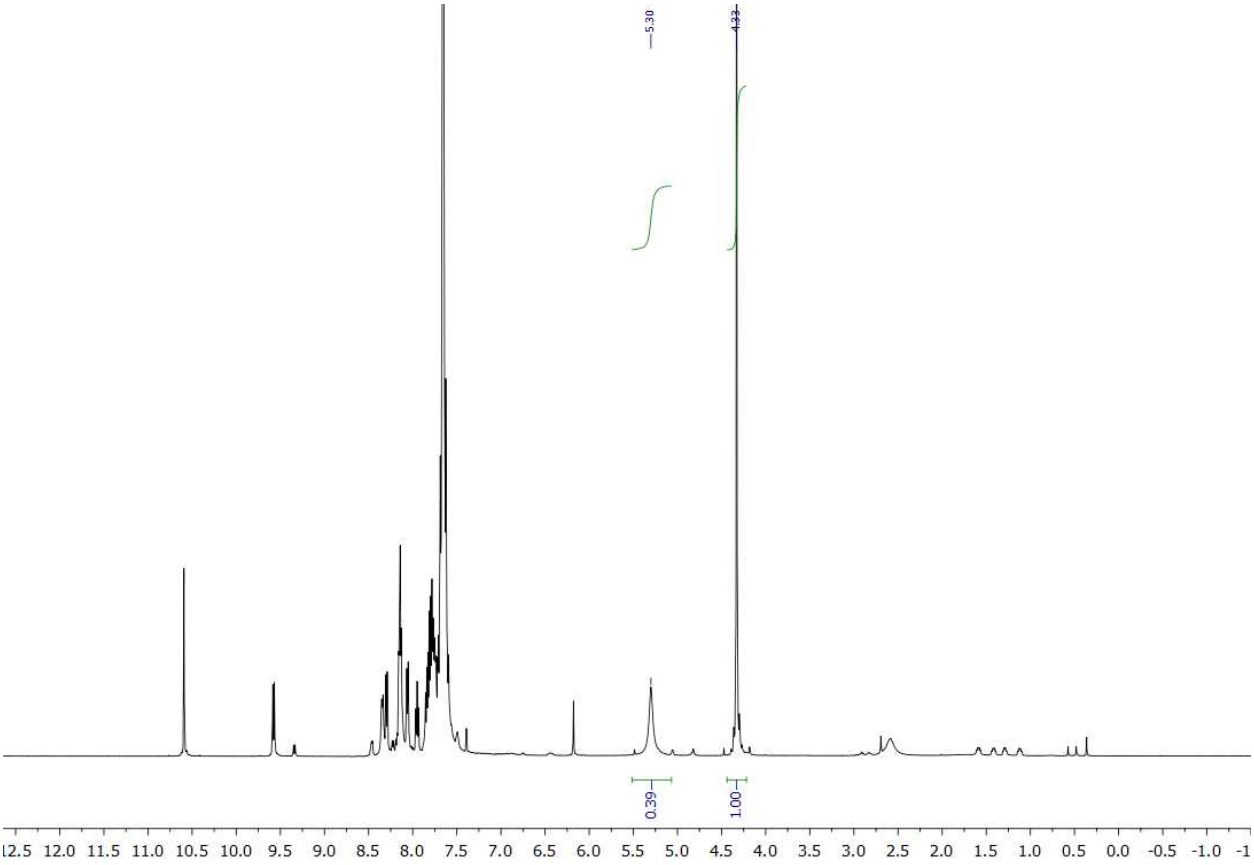

Figure 2.11 ^{1}H NMR (500 MHz, $CDCl_3$) analysis of the reaction mixture from the dehydrogenative coupling of 1-naphthalenemethanol

2.3.2.7 2-naphthalenemethanol

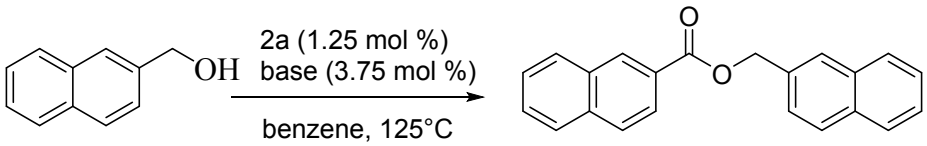

A 15 mL reaction vessel was oven-dried and filled with 2a (4.1 mg, 6.25 μmol, 1.25 mol%), potassium tert-butoxide (2.1 mg, 18.75 μmol, 3.75 mol%), 2-naphthalenemethanol (79.1 mg, 0.5 mmol), and benzene (0.7 mL) in a glovebox filled with nitrogen. After sealing the vessel with a screw cap lined with PTFE, the glovebox was opened, and the reaction vessel was brought out of the box. An argon balloon was attached to maintain an inert atmosphere. It was then heated to 125 °C for 24 hours. After the reaction was completed, an internal standard of 20 μL of nitromethane was introduced. Then it was passed through wool and Celite. The resultant mixture was cleaned with deuterated chloroform and put in a tube for an NMR study to be performed on the sample. NMR yield: 74%

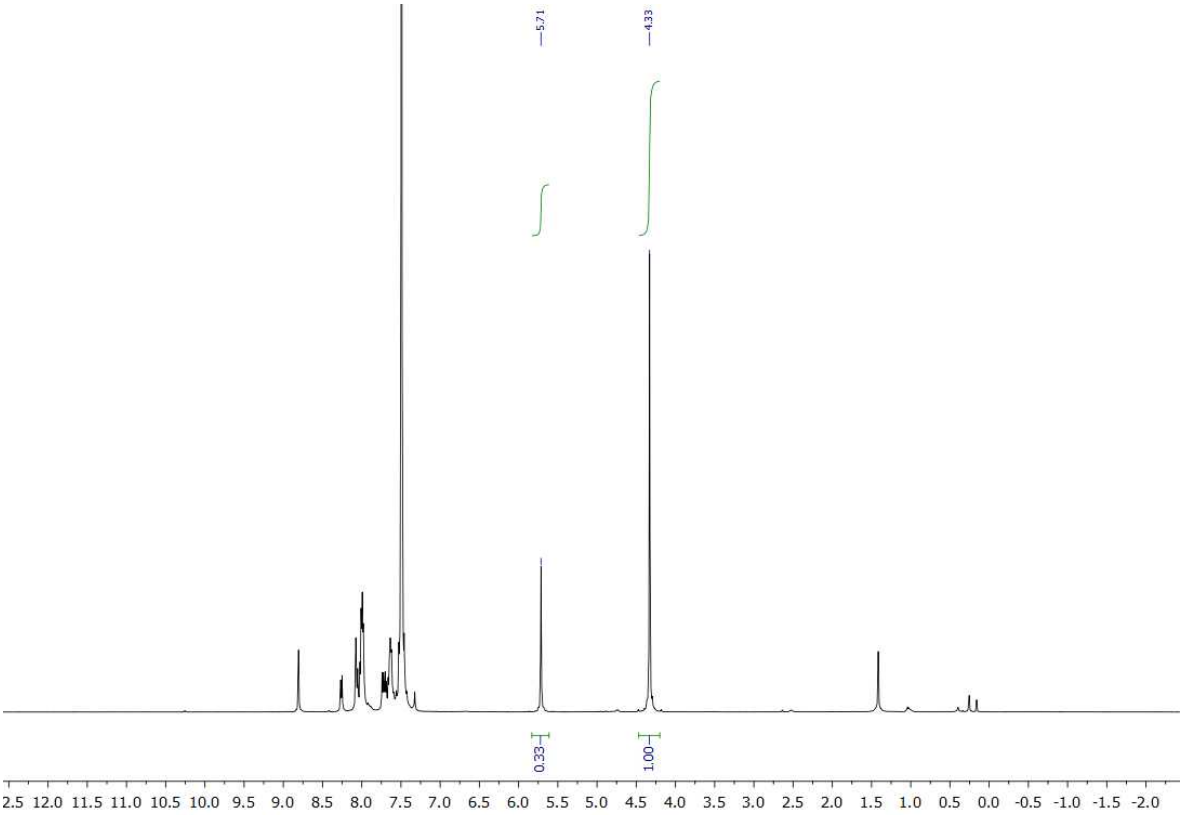

Figure 2.12 ^{1}H NMR (500 MHz, $CDCl_3$) analysis of the reaction mixture from the dehydrogenative coupling of 2-naphthalenemethanol

2.3.2.8 3-FluoroBenzyl Alcohol

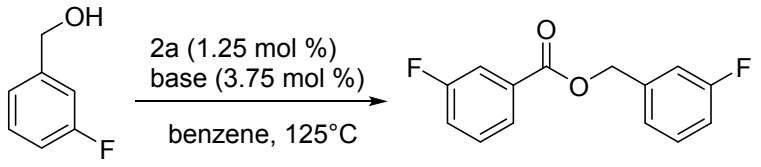

A 15 mL reaction vessel was oven-dried and filled with 2a (4.1 mg, 6.25 µmol, 1.25 mol%), potassium tert-butoxide (2.1 mg, 18.75 µmol, 3.75 mol%), 3-fluorobenzyl alcohol (63.1 mg, 0.5 mmol), and benzene (0.7 mL) in a glovebox filled with nitrogen. After sealing the vessel with a screw cap lined with PTFE, the glovebox was opened, and the reaction vessel was brought out of the box. An argon balloon was attached to maintain an inert atmosphere. It was then heated to 125 °C for 24 hours. After the reaction was completed, an internal standard of 20 µL of nitromethane was introduced. Then it was passed through wool and Celite. The resultant mixture was cleaned with deuterated chloroform and put in a tube for an NMR study to be performed on the sample. NMR yield: 98%

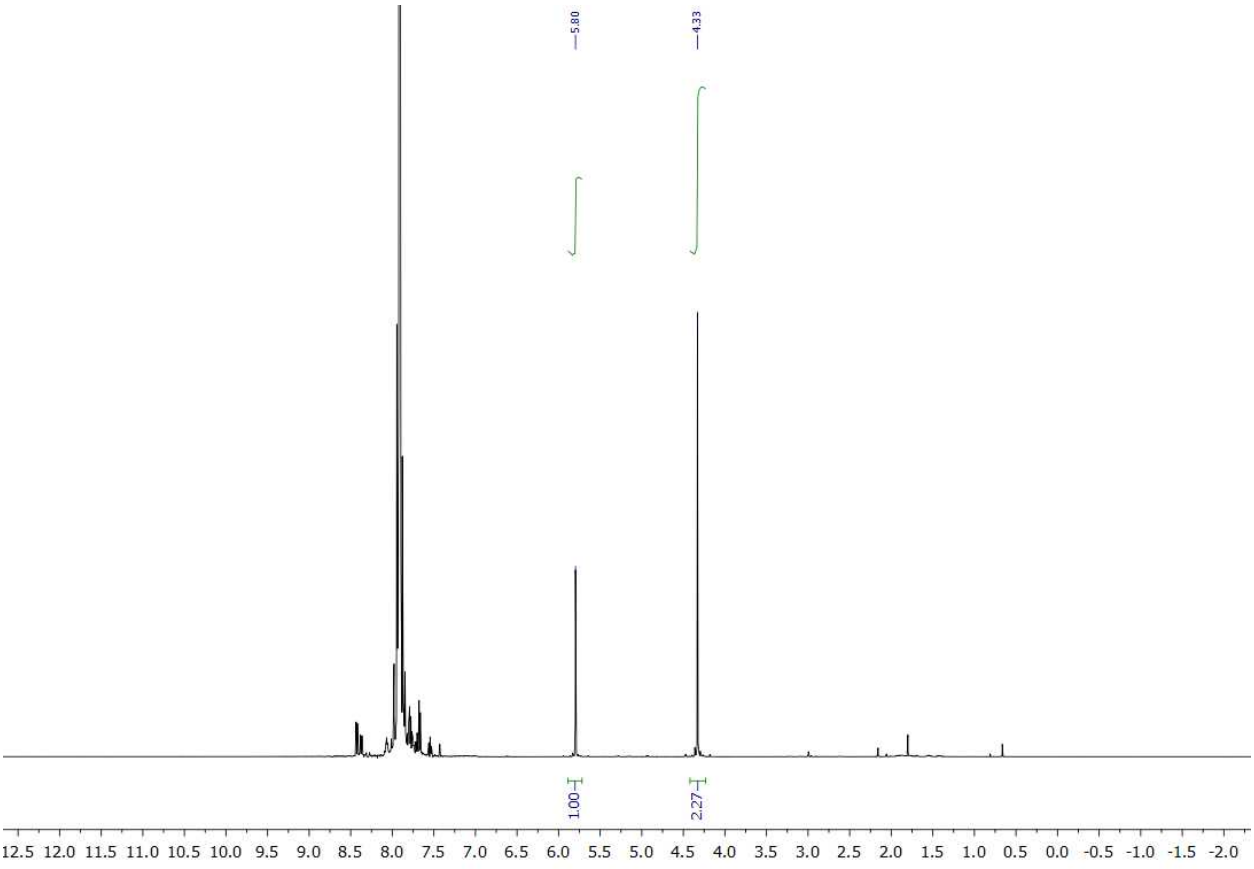

Figure 2.13 ^{1}H NMR (500 MHz, $CDCl_3$) analysis of the reaction mixture from the dehydrogenative coupling of 3-Fluoro benzyl alcohol

2.3.2.9 3-(trifluoromethyl) Benzyl Alcohol

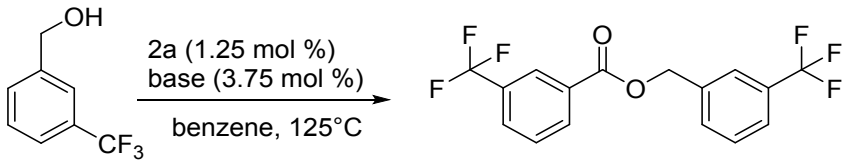

A 15 mL reaction vessel was oven-dried and filled with 2a (4.1 mg, 6.25 μmol, 1.25 mol%), potassium tert-butoxide (2.1 mg, 18.75 μmol, 3.75 mol%), 3-(trifluoromethyl) Benzyl Alcohol (88.1 mg, 0.5 mmol), and benzene (0.7 mL) in a glovebox filled with nitrogen. After sealing the vessel with a screw cap lined with PTFE, the glovebox was opened, and the reaction vessel was brought out of the box. An argon balloon was attached to maintain an inert atmosphere. It was then heated to 125 °C for 24 hours. After the reaction was completed, an internal standard of 20 μL of nitromethane was introduced. Then it was passed through wool and Celite. The resultant mixture was cleaned with deuterated chloroform and put in a tube for an NMR study to be performed on the sample. NMR yield: 95%

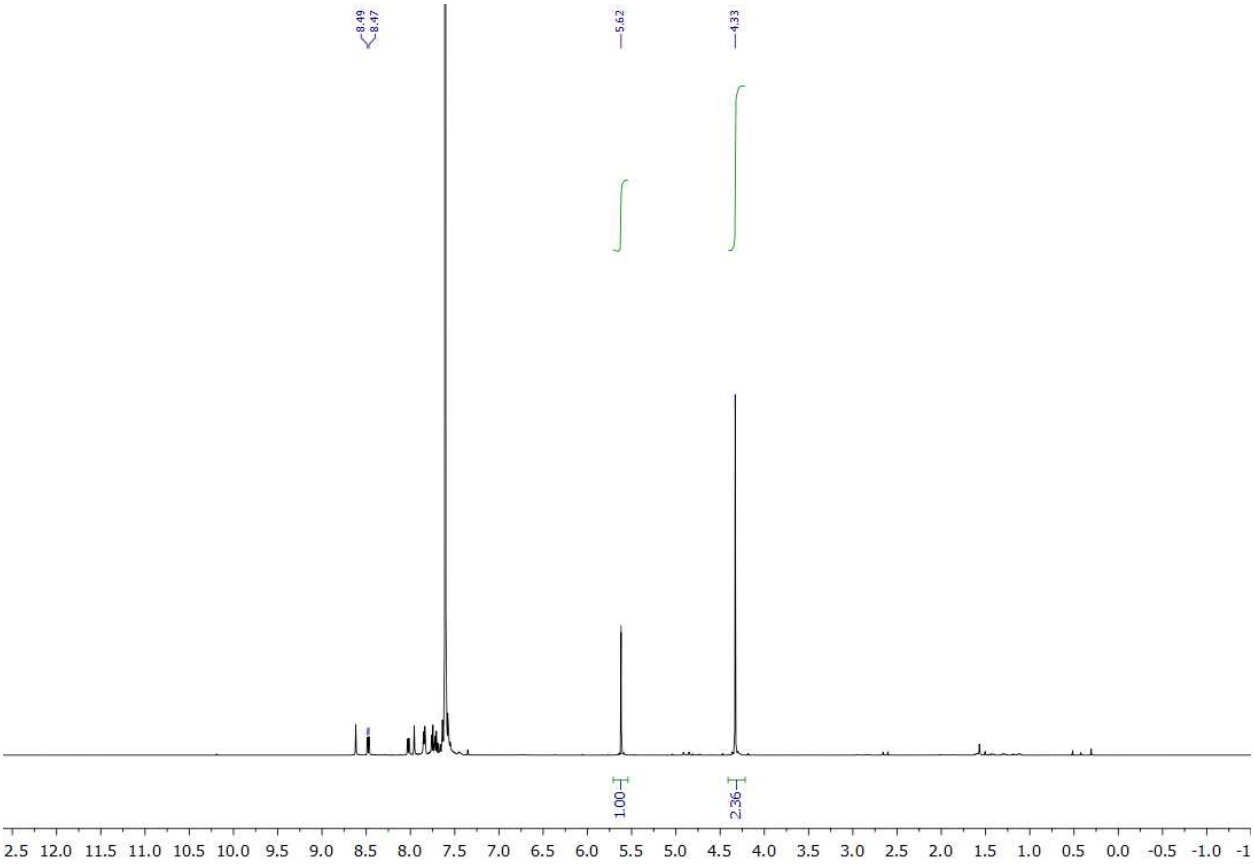

Figure 2.14 ^{1}H NMR (500 MHz, $CDCl_3$) analysis of the reaction mixture from the dehydrogenative coupling of 3-(trifluoromethyl) benzyl alcohol

2.3.2.10 3,5-bis(trifluoromethyl) benzyl alcohol

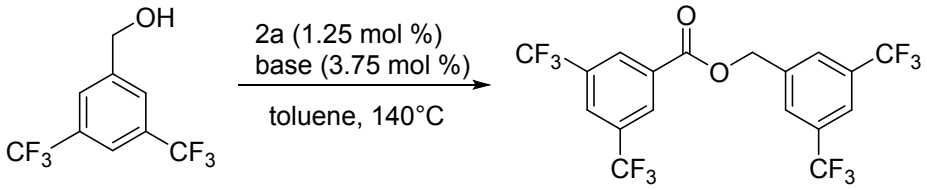

A 15 mL reaction vessel was oven-dried and filled with 2a (4.1 mg, 6.25 μmol, 1.25 mol%), potassium tert-butoxide (2.1 mg, 18.75 μmol, 3.75 mol%), 3,5-bis(trifluoromethyl) benzyl alcohol (122.1 mg, 0.5 mmol), and toluene (0.7 mL) in a glovebox filled with nitrogen. After sealing the vessel with a screw cap lined with PTFE, the glovebox was opened, and the reaction vessel was brought out of the box. An argon balloon was attached to maintain an inert atmosphere. It was then heated to 140 °C for 24 hours. After the reaction was completed, an internal standard of 20 μL of nitromethane was introduced. Then it was passed through wool and Celite. The resultant mixture was cleaned with deuterated chloroform and put in a tube for an NMR study to be performed on the sample. NMR yield: 58%

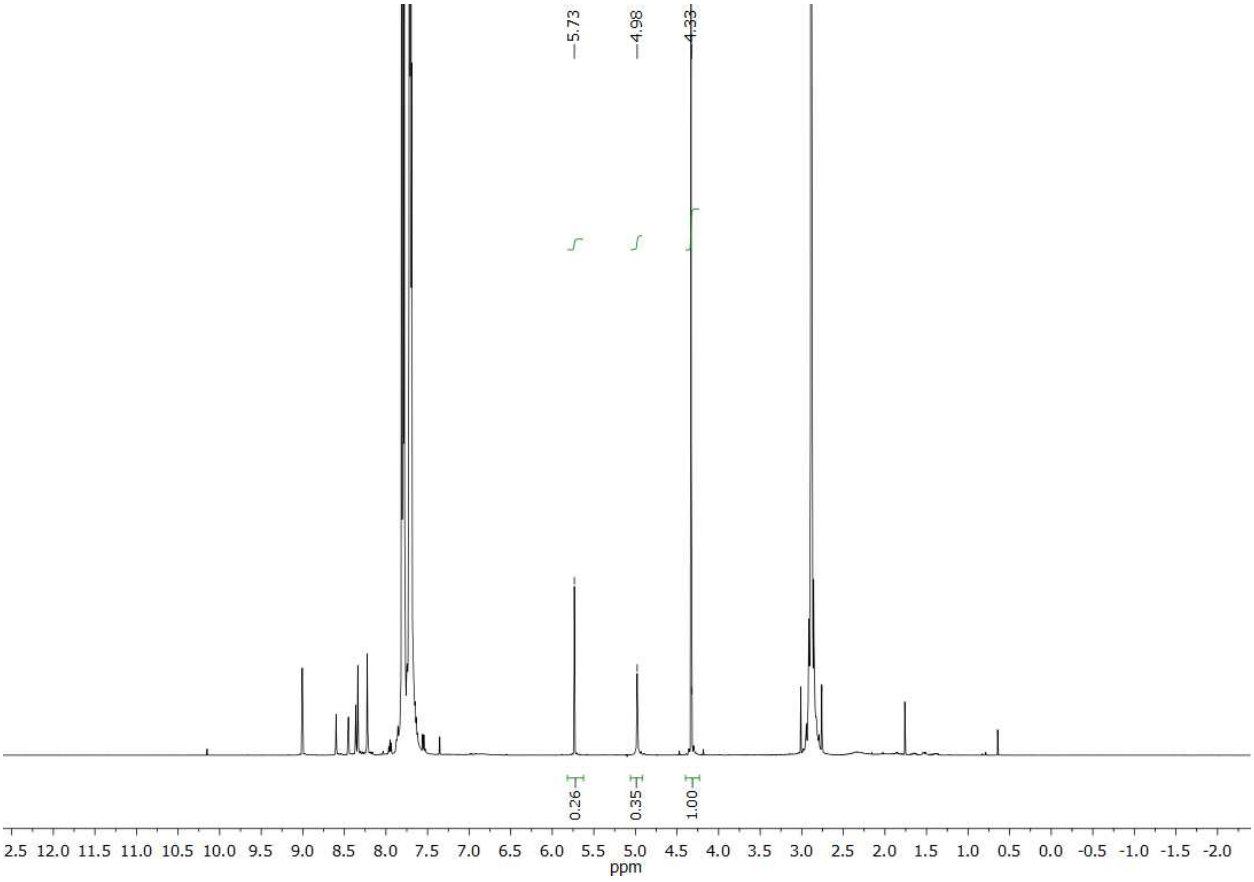

Figure 2.15 ^{1}H NMR (500 MHz, $CDCl_3$) analysis of the reaction mixture from the dehydrogenative coupling of 3,5-bis(trifluoromethyl) benzyl alcohol

2.3.2.11 3-fluoro-5-(trifluoromethyl) benzyl alcohol

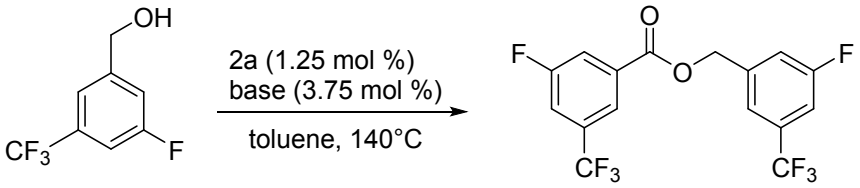

A 15 mL reaction vessel was oven-dried and filled with 2a (4.1 mg, 6.25 μmol, 1.25 mol%), potassium tert-butoxide (2.1 mg, 18.75 μmol, 3.75 mol%), 3-fluoro-5-(trifluoromethyl) benzyl alcohol (97.1 mg, 0.5 mmol), and toluene (0.7 mL) in a glovebox filled with nitrogen. After sealing the vessel with a screw cap lined with PTFE, the glovebox was opened, and the reaction vessel was brought out of the box. An argon balloon was attached to maintain an inert atmosphere. It was then heated to 140 °C for 24 hours. After the reaction was completed, an internal standard of 20 μL of nitromethane was introduced. Then it was passed through wool and Celite. The resultant mixture was cleaned with deuterated chloroform and put in a tube for an NMR study to be performed on the sample. NMR yield: 45%

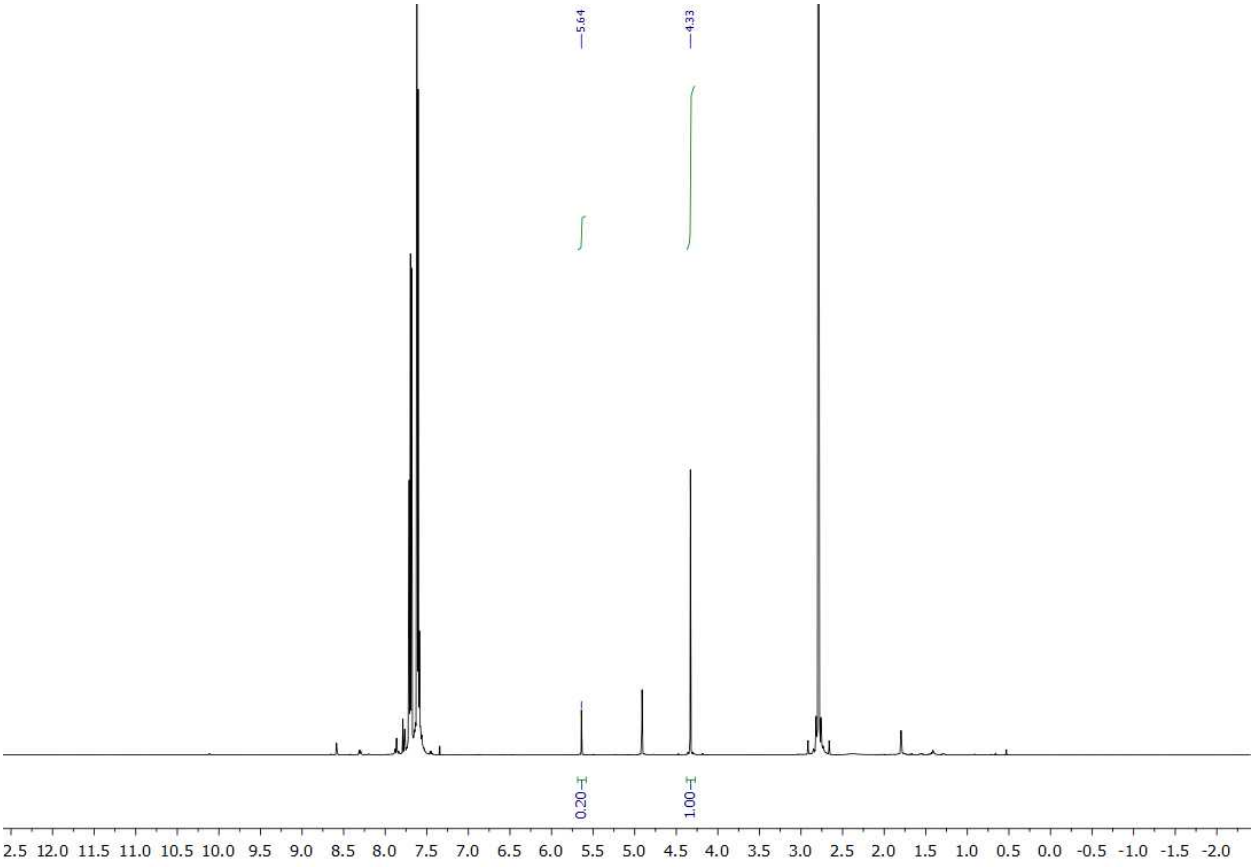

Figure 2.16 ^{1}H NMR (500 MHz, $CDCl_3$) analysis of the reaction mixture from the dehydrogenative coupling of 3-fluoro-5-(trifluoromethyl) benzyl alcohol

2.3.2.12 1-octanol

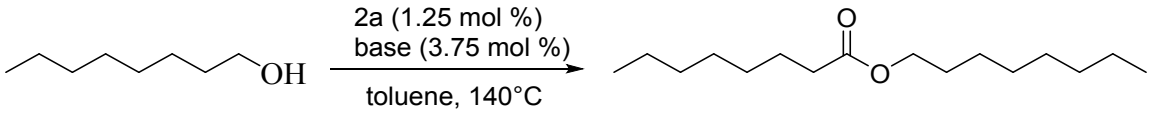

A 15 mL reaction vessel was oven-dried and filled with 2a (4.1 mg, 6.25 μmol, 1.25 mol%), potassium tert-butoxide (2.1 mg, 18.75 μmol, 3.75 mol%), 1-octanol (65.1 mg, 0.5 mmol), and toluene (0.7 mL) in a glovebox filled with nitrogen. After sealing the vessel with a screw cap lined with PTFE, the glovebox was opened, and the reaction vessel was brought out of the box. An argon balloon was attached to maintain an inert atmosphere. It was then heated to 140 °C for 24 hours. After the reaction was completed, an internal standard of 20 μL of nitromethane was introduced. Then it was passed through wool and Celite. The resultant mixture was cleaned with deuterated chloroform and put in a tube for an NMR study to be performed on the sample. NMR yield: 84%

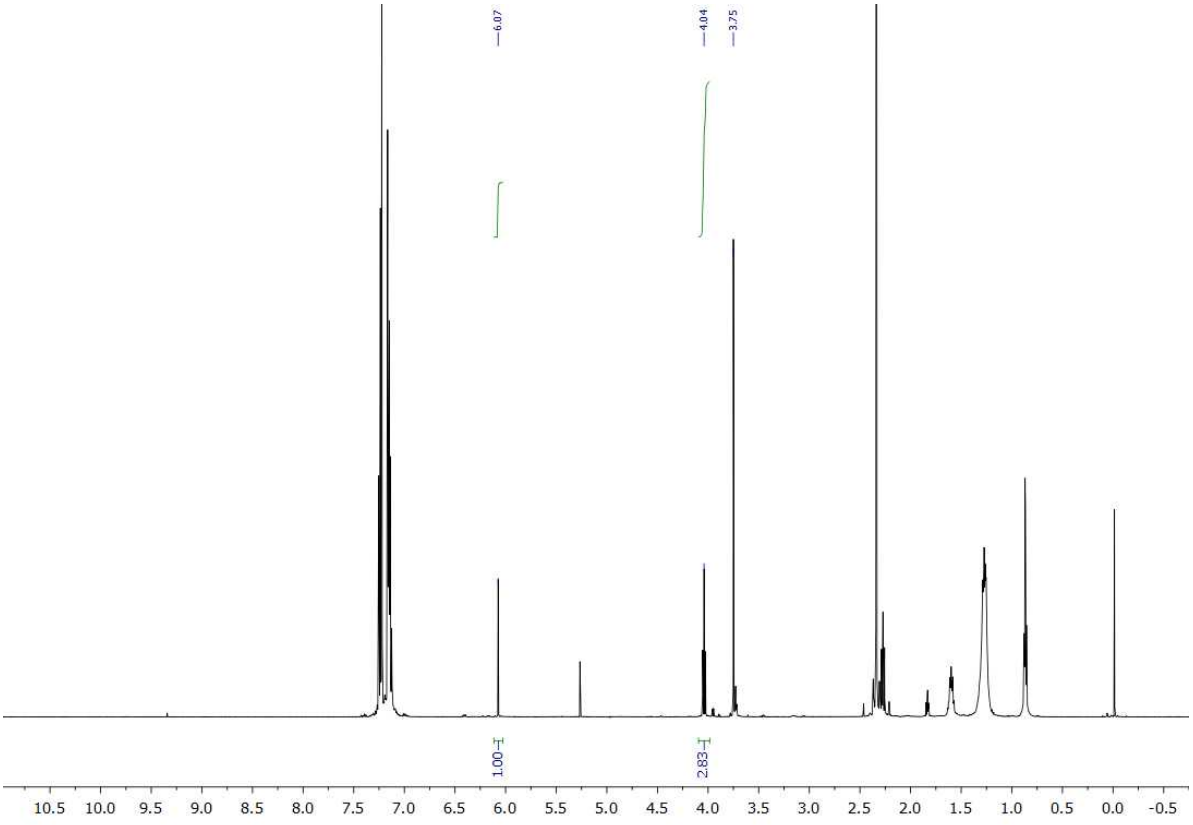

Figure 2.17 ^{1}H NMR (500 MHz, $CDCl_3$) analysis of the reaction mixture from the dehydrogenative coupling of 1-octanol.

CHAPTER 3

RESULTS AND DISCUSSION

3.1 Synthesis of ^{iPr}PPPBF Ligand and its Cobalt Complex

The design of ligands is a key factor influencing the catalytic performance of metal complexes. The catalytic activity of base metal complexes in the dehydrogenative homocoupling of primary alcohols to esters is quite rare, with only a handful of examples reported.

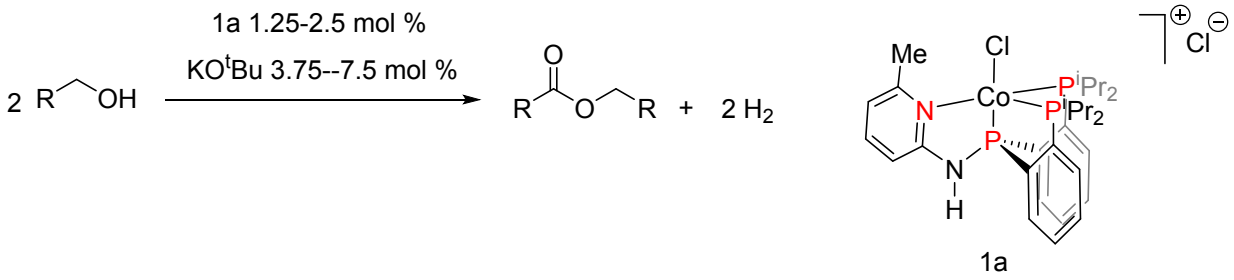

Scheme 3.1 KO^{t}Bu-Catalyzed Dehydrogenative Coupling of Primary Alcohols

To advance the development of first-row transition metal catalysts, a tripodal tetradentate ligand, ^{iPr}PPPN^{H}Py^{Me}, was synthesized in our research group and used in cobalt complex formation. This multidentate ligand incorporates strong-field phosphine donors that stabilize low-spin metal centers. (Scheme 3.1). A catalytic system involving a cobalt complex **1a** supported by ^{iPr}PPPN^{H}Py^{Me} ligand and KO^{t}Bu was developed for efficient transformation of primary aliphatic and aromatic alcohols to esters.

In this thesis, we present an alternative catalytic system based on the pincer phosphine ligand ^{iPr}PPPBF ligand and its cobalt-coordinated complex. This ligand is characterized by three strong phosphorus donors, with one linked to the electron-rich benzofuran group. The newly developed

catalytic system demonstrates catalytic efficiencies for ester formation similar to those observed with $^{iPr}PPPN^{H}Py^{Me}$.

The tridentate pincer ^{iPr}PPPBF ligand **2** was synthesized through a three-step process. The first step product (2-bromophenyl) diisopropylphosphine is available in our lab from previous work, and used as is. (Step 1) In the following step, (2-bromophenyl) diisopropylphosphine is activated with 1 equiv of n-butyllithium via lithium-halogen exchange followed by nucleophilic substitution at the phosphorus center of $P(OPh)_3$, to give a phosphine oxide intermediate. (Step 2) In the final step, benzofuran is added to the previous obtained reaction slurry in the presence of ^{n}BuLi and tetrahydrofuran (THF) at -78 °C. This step facilitates the formation of the target pincer type ^{iPr}PPPBF ligand 2, with the yield of %.

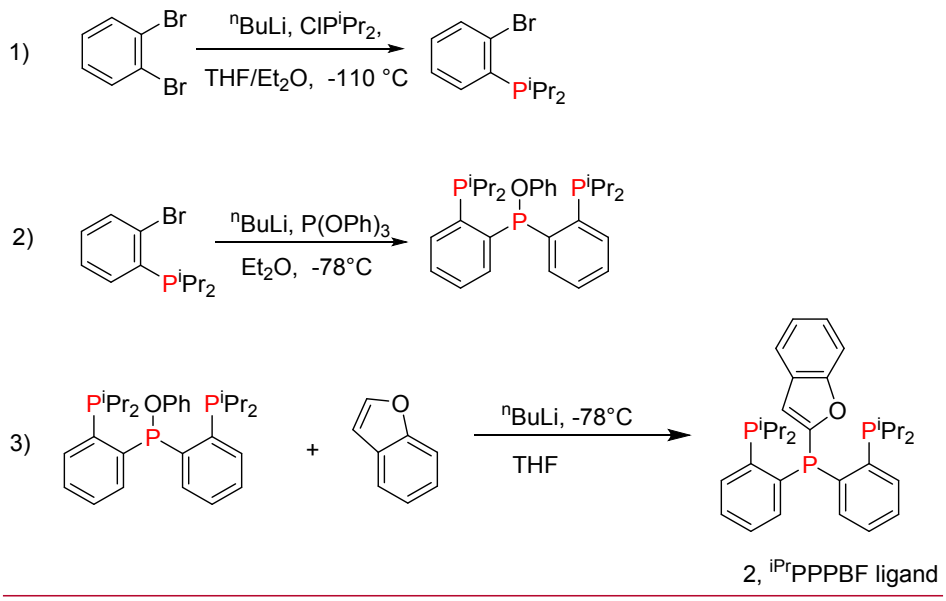

Scheme 3.2 Synthesis of ^{iPr}PPPBF Ligand 2

The $^{31}P\{^{1}H\}$ NMR spectrum of **2** contains three sharp resonances at 298 K: a doublet of doublets at −32.6 ppm is assigned to the central phosphine, and two doublets at −1.6 ppm are assigned to the terminal phosphines in a 1:1 ratio, with a $^{31}P–^{31}P$ coupling constant of 162 Hz.

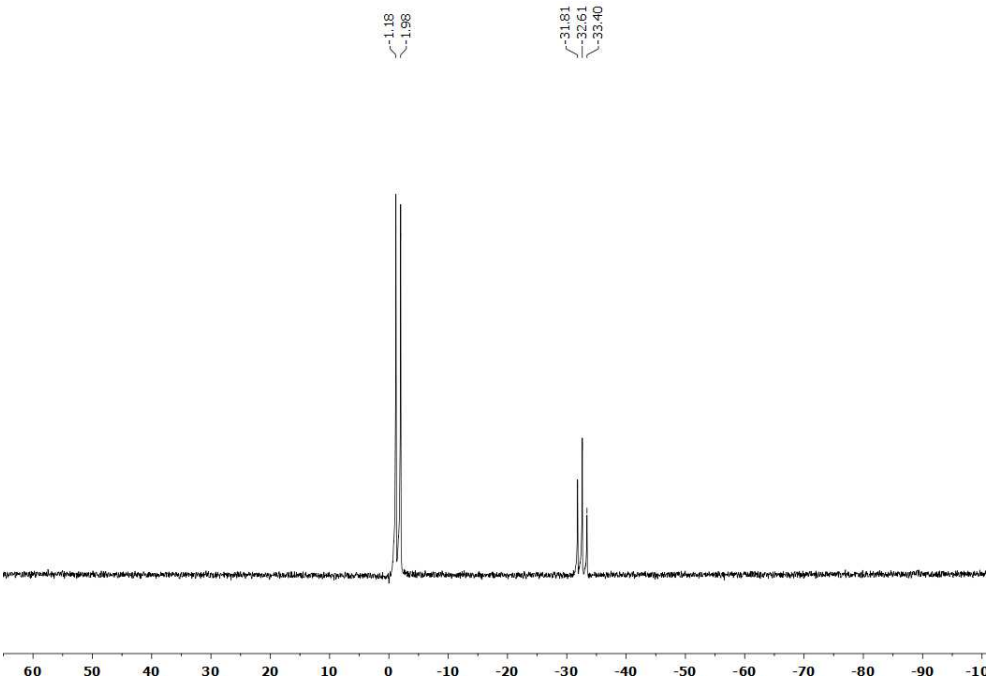

Figure 3.1 $^{31}P\{^{1}H\}$NMR spectra (121 MHz) of **2** in $CDCl_3$

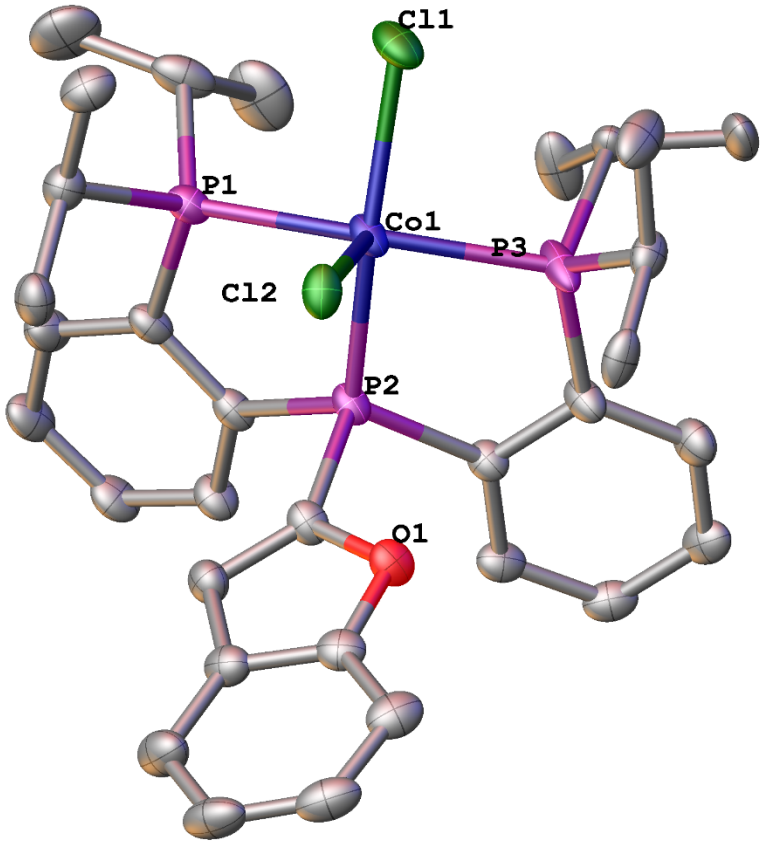

Figure 3.2 Xray Crystal Structure of [(^{iPr}PPPBF)$CoCl_2$] (**2a**). 50% probability of thermal ellipsoids; H atoms are omitted except for that of the N-H linker.

The treatment of **2** with $CoCl_2$ in tetrahydrofuran afforded [(^{iPr}PPPBF)$CoCl_2$] (**2a**) as a dark-red powder in 86% isolated yield. To obtain a solid-state molecular structure, **2a** was crystallized as dark-red needles by vapor diffusion of diethyl ether into a concentrated dichloromethane solution. The X-ray structure revealed a pseudo square pyramidal geometry on the Co center, with the Cl2 atoms in the axial positions and the phosphines (P1, P2 and P3) and Cl1 donor in the equatorial positions. The three phosphorus donor atoms are arranged in a pincer-like configuration around the metal, stabilizing it from three sides. This tridentate nature provides a highly stable chelating environment for the metal. The diisopropyl substituents on the phosphine atoms provide significant

steric bulk, which not only shields the metal center from unwanted interactions but also enhances the ligand's electron-donating ability. The benzofuran group in the cobalt complex is linked to a phosphorus atom P2, acting as a non-coordinating ligand that stabilizes the structure while preserving its aromaticity. Its position and steric bulk influence the electronic environment and geometry around the cobalt center, potentially affecting the complex's reactivity.

3.2 Catalytic Dehydrogenative Coupling of Primary Alcohols

Reaction optimization was carried out taking benzyl alcohol as a model substrate for dehydrogenative homocoupling to benzyl benzoate. Complex **2a** were used as pre-catalysts (Scheme 3.3). To optimize a reaction, conditions such as temperature, pre-catalyst loading, additive loading and solvent were considered. Optimization began at 80 °C in a 100 mL pressure vessel under a nitrogen atmosphere, yielding only 62% (Table 3.1, entry 1). Raising the temperature to 125 °C resulted in an impressive, nearly quantitative conversion of benzyl alcohol to benzyl benzoate (>99% yield, Table 3.1, entry 3). Repeating the reaction in a 15 mL reaction tube with an argon flow system achieved a 98% yield (Table 3.1, entry 3). In the absence of 2a, only trace amounts of product were detected, confirming its catalytic role (Table 3.1, entry 10), and no esterification occurred without a base, indicating its crucial role (Table 3.1, entry 11). Substituting benzene with toluene, THF, or 1,4-dioxane led to reduced yields of 72%, 42%, and 35%, respectively (Table 3.1, entries 5–7). KO^{t}Bu and NaO^{t}Bu proved to be more effective bases for esterification than NaOMe (Table 3.1, entries 8 and 9). Thus, the optimized conditions included KOtBu or NaOtBu as a base, benzene as a solvent, and a temperature of 125 °C.

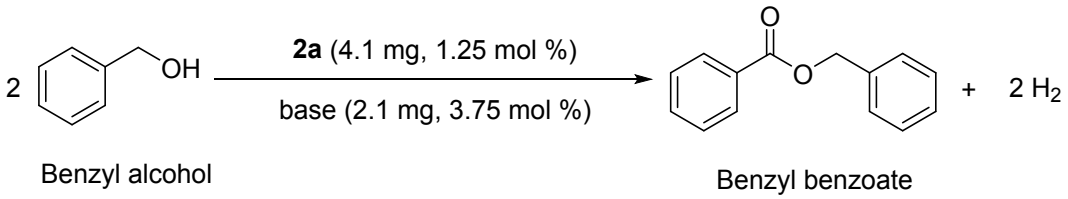

Scheme 3.3 Dehydrogenative homocoupling of benzyl alcohol to benzyl benzoate

Table 3.1 Optimizations of Reaction Conditions [a,]

Entry	Catalyst	Base	Solvent	Temp (°C)	Yield (%) [b]
1	**2a**	KO^{t}Bu	benzene	80	62
2	**2a**	KO^{t}Bu	benzene	110	78
3	**2a**	KO^{t}Bu	benzene	125	>99, 98[c]
4	**2a**	KO^{t}Bu	toluene	110	61
5	**2a**	KO^{t}Bu	toluene	125	72
6	**2a**	KO^{t}Bu	THF	125	42
7	**2a**	KO^{t}Bu	1,4-dioxane	125	35
8	**2a**	NaO^{t}Bu	benzene	125	95
9	**2a**	NaOMe	benzene	125	82
10	_	KO^{t}Bu	benzene	125	3
11	**2a**	–	benzene	125	0
12	**2a**	KO^{t}Bu	benzene	125	94 [d]

[a] Reaction conditions: **2a** (1.25 mol %), base (3.75 mol %), benzyl alcohol (0.5 mmol), and solvent (0.7 mL) were heated in a sealed 100 mL reaction tube for 24 h. [b] Yields were determined by ^{1}H NMR analysis of the crude reaction mixture with nitromethane as an internal standard. [c] The reaction

mixture was heated in a 15 mL reaction tube with an argon balloon on top for 24 h. [d] Mercury (125 mg) was added to the reaction.

Table 3.2 Dehydrogenative homocoupling of primary alcohols catalyzed by cobalt complex **2a** and KO^{t}Bu[a]

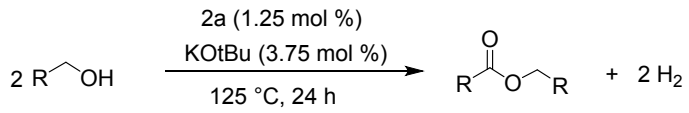

Entry	Product	Entry	Product	Entry	Product
1	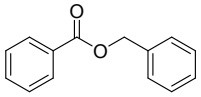	5	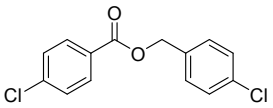	9	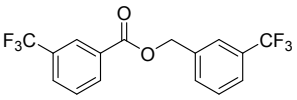
	97%		83%		95%
2	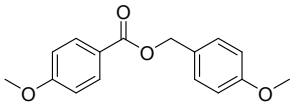	6	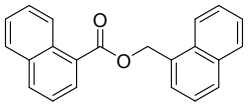	10	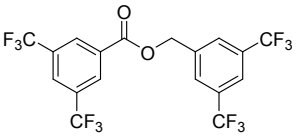
	98%		87%		58%
3	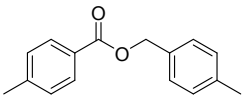	7	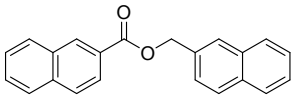	11	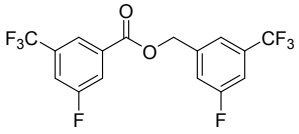
	99%		74%		45%
4	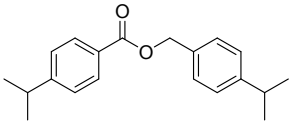	8	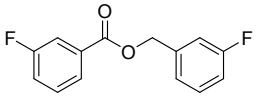	12	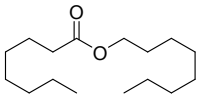
	94%		98%		84%

[a]Reaction conditions: alcohol (0.5 mmol), **2a** (1.25 mol %), KOtBu (3.75 mol %), benzene (0.7 mL) were heated in 15 mL reaction tube with argon balloon on top at 125 °C for 24 h. [b]Yields were determined by ^{1}H NMR with nitromethane or 1,3,5-trimethoxy benzene as internal standard.

3.3 Catalytic Dehydrogenative Coupling of Primary Alcohols to Esters

After having optimized conditions, various primary alcohol substrates were examined for dehydrogenative homocoupling to esters. At first, aromatic primary alcohols having electron releasing groups like OMe, Me, and iPr at para position were carried out for esterification and a smooth reactivity with an NMR yield of 97% to 99% was recorded (Table 3.2, entry 2 to 4). In addition, primary aromatic alcohol substrates with an electron withdrawing group Cl at para position also showed good reactivity and converted to their corresponding esters with an isolated yield of 83% (Table 3.2, entry 5). Interestingly, excellent yield was obtained from sterically hindered substrates 1-naphthalenemethannol (NMR yield of 87%) (Table 3.2, entry 6). A comparable yield of 74% was obtained from 2-naphthalenemethanol (Table 3.2, entry 7). Interestingly, meta-substituted substrates such as 3-fluorobenzyl alcohol and 3-trifluoromethyl benzyl alcohol both showed great yields of 98% and 95%, respectively (Table 3.2, entry 8 and 9). 3,5-trifluoromethyl benzyl alcohol and 3-fluoro-5-trifluoromethyl benzyl alcohol generated relatively lower yield of 58% and 45%, respectively (Table 3.2, entry 10 and 11). Aliphatic 1-octanol gives 84% yield (Table 3.2, entry 12).

3.4 Homogeneity Test of the reaction system

To assess whether the catalysis is homogeneous or heterogeneous, the dehydrogenative homocoupling of benzyl alcohol to benzyl benzoate was performed with 100 equivalents of mercury relative to complex **2a**. (Section 2.3.1) Analysis of the product showed a 94% yield, indicating that mercury did not hinder reactivity and supporting the presence of a homogeneous catalytic system.

3.5 Proposed Reaction Mechanism

Table 3.3 Effect of KO^{t}Bu Loadings on Dehydrogenative homocoupling of Benzyl Alcohol to benzyl benzoate[a,b]

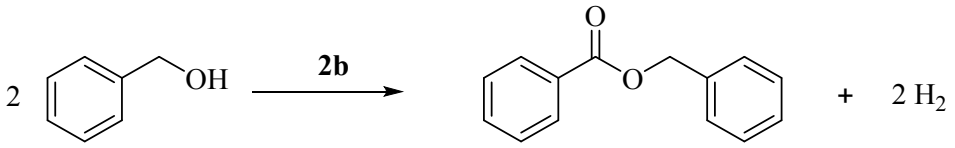

Entry	**2b**. (mol%)	KO^{t}Bu (mol%)	Yield[b] (%)
1	1.25	0	0
2	1.25	1.25	3
3	1.25	2.5	65
4	1.25	3.125	83
5	1.25	3.75	97

[a]Reaction conditions: benzyl alcohol (0.5 mmol), **2b** (1.25 mol%), KO^{t}Bu, benzene (0.70 mL) were heated in 100 mL pressure vessel, 125 °C, 24 h. [b]NMR yield using nitromethane as internal standard.

The roles of KO^{t}Bu were examined by carrying out reactions loaded with various ratios of complex **2b** and KO^{t}Bu (Table 3.3, entry 1 to 5). Without KO^{t}Bu, no esterification was observed (Table 3.3, entry 1). A 3% yield was achieved when using 1 equivalent of KO^{t}Bu (1.25 mol%) for esterification (Table 3.3, entry 2). This limited yield likely results from the minimal amount of KO^{t}Bu available, which is only sufficient to activate the Co precatalyst. However, this activation appears insufficient to complete all steps necessary for full esterification, leading to the modest 3% yield. In contrast, an impressive 65% yield was obtained with 2.5 mol% KO^{t}Bu (Table 3.3, entry 3), highlighting the additional crucial roles of KO^{t}Bu beyond merely precatalyst activation.

It was observed that esterification reactions produced small amounts of aldehydes as byproducts. Interestingly, KO^{t}Bu alone was observed to catalyze the Tishchenko coupling of aldehydes to form esters under mild conditions, aligning with our previous findings.[20] When the reaction was performed with 1 equivalent of alcohol added to the aldehyde at room temperature, only trace ester formation was detected, yielding a low 3% and suggesting that alcohol may inhibit Tishchenko coupling. Therefore, we propose that the reaction pathway involves initial dehydrogenation followed by KO^{t}Bu-catalyzed Tishchenko coupling (Scheme 3.4).

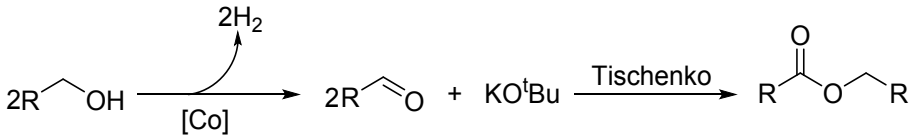

Scheme 3.4 Probable pathway for dehydrogenative homocoupling of alcohols to esters

CONCLUSION

In the relentless pursuit of greener chemical processes, our journey has led us to a groundbreaking discovery: a new and effective catalytic system for the acceptorless dehydrogenative coupling of primary alcohols to esters. The cornerstone of this invention is a beautiful pair – a pincer cobalt complex (2a) and potassium tert-butoxide (KO^tBu). This dynamic partnership has been remarkably productive; diverse primary alcohols have been converted to their corresponding esters under optimized conditions.

As the central metal in our complex, cobalt was not chosen randomly to test the waters. Cobalt is an earth-abundant metal that provides an exciting and sustainable solution to using precious metal catalysts in catalysis while shifting focus to the first-row transition metals. Using cobalt, a base metal in our system shows that if well-designed, base metals can even outcompete precious metals. The pincer ligand structure around the cobalt center is indeed one of the impressive yet overlooked aspects of our catalyst. The complex's geometry and electronic characteristics are perfect for the significant steps of the catalytic process. As we continue to develop the mechanistic understanding of these reactions, it is clear that ligand design plays a central role in facilitating the initial dehydrogenation of the alcohol and subsequent coupling processes.

Another striking feature of our catalytic system is its reasonably high scope of applicability. The scope of substrates includes aromatic and aliphatic primary alcohols, and the system manages them effectively. It is not sensitive to electron-donating or electron-withdrawing substituents in aromatic substrates and, therefore, is a versatile tool in the synthetic chemist working bench.

Our methodology is incredibly insightful in an era where sustainability defines the operations of businesses and organizations. The reaction only has hydrogen gas as the byproduct, which makes it a paragon of atom economy. Not only does it help to minimize waste, but it also presents fantastic opportunities for hydrogen production as a valuable side product. This dual-purpose aspect of the reaction is most attractive in a world that is gradually tilting towards accepting hydrogen as an efficient and clean energy carrier.

Our catalytic system does not only produce esters but also forms a link between renewable feedstock and valuable chemical commodities. Primary alcohols can be sourced from biomass or fermentation processes, and our proposed system will convert these feedstocks directly into commercially valuable ester products. Amid the challenges brought on by climate change and increasing scarcity of resources, such technologies that allow for the valorization of biomass-derived feedstocks will be instrumental in defining the chemical industry of the future.

We have much further to go, even though we have made significant progress. This methodology has a lot of potential that can be used to optimize the technique further and expand its usage. Further modifications of the pincer ligand and other supporting ligands could enhance the catalyst performance. We might even pave the way for asymmetric transformations to make new ways of forming chiral esters. Since the present system can form aldehydes as intermediates, we are excited about the potential to synthesize tandem reactions. It is easy to conceptualize adding the dehydrogenation step to aldol condensation or reductive amination - the potential to make a variety of complex architectures of molecules in one pot is tantalizing. It is also possible to go even further and look for even more complicated and functionalized primary alcohols that could extend the synthetic applicability of the reported catalytic system to other terrains.

The application of our work extends far beyond ester synthesis. Showing that a base metal can also play a vital role in a field dominated by noble metals is revolutionary because it brings more economical and sustainable approaches to organic synthesis and other industrial applications of catalysis. Furthermore, based on the knowledge we obtained, especially the function of the base and the suggested reaction mechanism, it may be possible to develop new catalyst systems for similar transformations. Such a ripple effect may open up new horizons in diverse fields of synthetic chemistry, which might fundamentally change the traditional synthetic strategies for building up complex organic molecules.

As we prepare to enter a new age of green chemistry, our cobalt-catalyzed system is much more than an innovative strategy for esterification. It's a testament to the power of interdisciplinary research in addressing complex chemical challenges, drawing upon principles from organometallic chemistry, homogeneous catalysis, green chemistry, and even enzyme catalysis. There are lots of promising opportunities in sight. From developing even more active and selective catalysts to exploring new applications in complex molecule synthesis, the potential impact of this work is far-reaching. Thus, the further development of such concepts as ours, associated with catalysis, will be even more critical in the face of global challenges related to sustainability and efficient usage of resources.

Consequently, the conceptualization to realization process of our synthetic chemistry work has not only delivered an impressive new synthetic methodology but also helped to define a new scientific direction of chemical synthesis and catalysis. As we continue to push the boundaries of what's possible with earth-abundant metal catalysts, we move closer to a future where efficient, sustainable processes are the norm in organic synthesis and industrial chemistry. This is just the start of the adventure, and even more exciting than what has been described so far lies ahead.

Our contribution is shaping the synthesis process and the chemical reactions behind it, pushing the boundaries of sustainable chemistry in every aspect, and facilitating a better future.

REFERENCES

Larock, R. C. *Comprehensive Organic Transformations*; VCH: New York, 1989.

Ogliaruso, M. A.; Wolfe, J. F. *Synthesis of Carboxylic Acids, Esters and Their Derivatives*; John Wiley & Sons Ltd: Hoboken, NJ, 1991.

Shieh, W. C.; Dell, S.; Repič, O. Nucleophilic Catalysis with 1,8-Diazabicyclo[5.4.0]undec-7-ene (DBU) for the Esterification of Carboxylic Acids with Dimethyl Carbonate. *J. Org. Chem.* **2002**, *67*(7), 2188-2191.

Intergovernmental Panel on Climate Change (IPCC). Climate Change 2021 – *The Physical Science Basis: Working Group I Contribution to the Sixth Assessment Report of the Intergovernmental Panel on Climate Change.* Cambridge University Press; 2023.

Doney, S. C.; Busch, D. S.; Cooley, S. R.; Kroeker, K. J. The Impacts of Ocean Acidification on Marine Ecosystems and Reliant Human Communities. *Annual Review of Environment and Resources* **2020**, 45, 83-112.

Shindell, D. T., Faluvegi, G., Koch, D. M., Schmidt, G. A., Unger, N., & Bauer, S. E. Improved Attribution of Climate Forcing to Emissions. *Sci* **2009**, *326*(5953), 716-718.

Chakraborty, S.; Piszel, P. E.; Brennessel, W. W.; Jones, W. D. A Single Nickel Catalyst for the Acceptorless Dehydrogenation of Alcohols and Hydrogenation of Carbonyl Compounds. *Organometallics* **2015**, *34*(21), 5203−5206.

Bielinski, E. A.; Förster, M.; Zhang, Y.; Bernskoetter, W. H.; Hazari, N.; Holthausen, M. C. Base-Free Methanol Dehydrogenation Using a Pincer-Supported Iron Compound and Lewis Acid Co-catalyst. *ACS Catal*. **2015**, *5*(4), 2404−2415.

Nguyen, D. H.; Trivelli, X.; Capet, F.; Paul, J. F.; Dumeignil, F.; Gauvin, R. M. Manganese Pincer Complexes for the Base-Free, Acceptorless Dehydrogenative Coupling of Alcohols to Esters: Development, Scope, and Understanding. *ACS Catal*. **2017**, 7(3), 2022−2032.

van Koten, G.; Timmer, K.; Noltes, J. G.; Spek, A. L. A novel type of Pt–C interaction and a model for the final stage in reductive elimination processes involving C–C coupling at Pt; synthesis and molecular geometry of [1,N,N′-η-2,6-bis{(dimethylamino)methyl}-toluene]iodoplatinum(II) tetrafluoroborate. *J. Chem. Soc., Chem. Commun*., **1978**, *6,* 250 – 252.

Moulton, C. J.; Shaw B. L. Transition metal–carbon bonds. Part XLII. Complexes of nickel, palladium, platinum, rhodium and iridium with the tridentate ligand 2,6-bis[(di-t-butylphosphino)methyl]phenyl. *J. Chem. Soc., Dalton Trans*., **1976**, *11,* 1020–1024.

Peris, E.; Crabtree, R. H. Key factors in pincer ligand design. *Chem. Soc. Rev.* **2018**, *47*(6), 1959-1968.

Choi, J.; Roy MacArthur, H. A.; Brookhart, M.; Goldman, S. A. Dehydrogenation and Related Reactions Catalyzed by Iridium Pincer Complexes. *Chem. Rev.* **2011**, *111*(3), 1761-1779.

Morales-Morales, D.; Jensen, C. M. *The Chemistry of Pincer Compounds*; Elsevier: 2007.

Deng, Q.; Melen, R. L.; Gade, L. H. Anionic Chiral Tridentate N-Donor Pincer Ligands in Asymmetric Catalysis. *Acc. Chem. Res*. **2014**, *47*(10), 3162-3173.

Gunanathan, C.; Milstein, D. Bond Activation and Catalysis by Ruthenium Pincer Complexes. *Chem. Rev*. **2014**, *114*(24), 12024-12087.

van Leeuwen, P. W.; Kamer, P. C.; Reek, J. N.; Dierkes, P. Ligand Bite Angle Effects in Metal-catalyzed C−C Bond Formation. *Chem. Rev.* **2000**, *100*(8), 2741-2770.

Younus, H. A.; Ahmad, N.; Su, W.; Verpoort, F. Ruthenium Pincer Complexes: Ligand Design and Complex Synthesis. *Coor. Chem. Rev.* **2014**, 276, 112-152.

Gandeepan, P.; Müller, T.; Zell, D.; Cera, G.; Warratz, S.; Ackermann, L. 3d Transition Metals for C–H Activation. *Chem. Rev.* **2019**, *119*(4), 2192-2452.

Paudel, K.; Pandey, B.; Xu, S.; Taylor, D. K.; Tyer, D. L.; Torres, C. L.; Gallagher, S.; Kong, L.; Ding, K. Cobalt-Catalyzed Acceptorless Dehydrogenative Coupling of Primary Alcohols to Esters. *Org. Lett*. **2018**, *20* (14), 4478-4481.